Proteomic Insights Into Anaplastic Meningioma Heterogeneity

Ines Cela

Lund, January 2026

LUND UNIVERSITY

LTH

FACULTY OF ENGINEERING

Master´s Thesis in Biomedical Engineering

Faculty of Engineering, LTH
Department of Biomedical Engineering

Supervisor: Melinda Rezeli

Acknowledgements

I would like to begin by thanking my supervisor, Melinda Rezeli, for her invaluable guidance, expertise and support throughout this project. I am deeply grateful for her constant availability, encouragement, and willingness to help at every stage of the project. Beyond her direct support with the project, I have also learned a great deal from her, for which I am sincerely thankful.

I would also like to thank Bálint Scheich and Katalin Dezső, the two researchers for providing the project idea, the meningioma samples, and the associated clinical information. I am grateful for their valuable insights into the project, responsiveness, and continued willingness to answer my questions and provide the information I needed.

Abstract

Meningiomas are the most common primary tumors of the central nervous system and show clinical heterogeneity across WHO grades. While grade 1 meningiomas are typically benign, grade 3 (anaplastic) meningiomas are rare, highly aggressive, and associated with poor prognosis. Current histopathological grading does not fully capture tumor biology, therefore molecular approaches are needed to better reflect disease behavior. Proteomic profiling provides insight into functional biological differences between tumor grades, but sample processing and analysis of formalin-fixed paraffin-embedded (FFPE) tissues remains challenging.

This study aimed to develop and implement a robust, high-throughput proteomics workflow for FFPE tissues and to apply the workflow to meningioma samples in order to characterize proteomic differences between grade 1 and grade 3 tumors, explore heterogeneity within high-grade meningiomas, and investigate associations with EZH2 expression. Multiple deparaffinization, protein extraction, and digestion methods were systematically evaluated using pilot tissues to optimize protein yield, reproducibility, and proteome coverage. The final workflow consisted of n-heptane/methanol deparaffinization, BeatBox-based protein extraction, and automated magnetic bead-based digestion on the KingFisher Apex platform.

The optimized protocol was applied to a cohort of 43 FFPE meningioma samples analyzed by data-independent acquisition mass spectrometry. Proteomic analysis revealed clear differences between grade 1 and grade 3 meningiomas, with high-grade tumors showing increased abundance of proteins involved in proliferation, DNA replication, RNA processing, and metabolic reprogramming. Pathway enrichment analyses confirmed a predominance of proliferative and biosynthetic pathways in grade 3 tumors, whereas grade 1 meningiomas were associated with homeostatic and cytoskeletal processes.

Unsupervised clustering further identified three distinct proteomic subgroups within grade 3 meningiomas, each associated with different biological pathways, EZH2 expression levels, and clinical outcomes. These findings demonstrate pronounced biological heterogeneity within high-grade meningiomas and highlight the potential of FFPE-based proteomics to refine tumor stratification beyond histological grading.

Table of Contents

Introduction

Meningiomas are the most common primary tumors of the central nervous system (CNS) in adults and are currently classified as grade 1 to 3 according to the World Health Organization (WHO) system (CNS WHO 5). Meningiomas of different grades are characterized by significantly different behavior. While grade 1 tumors are typically benign, grade 2 cases are characterized by intermediate behavior, while grade 3 meningiomas exhibit aggressive growth, high recurrence rates, and limited therapeutic options. However, the molecular mechanisms underlying this variability remain insufficiently understood. The WHO grade is currently determined by histopathological features (such as mitotic activity) and does not provide accurate prediction of the prognosis in a significant proportion of cases. Therefore, more accurate, but not generally available classification schemes were described in the last years, based on genome-wide DNA-methylation patterns, or multiomic approaches (Nassiri et al., 2021; Sahm et al., 2017). Proteomic profiling offers an opportunity to map functional biological differences between tumor grades, but FFPE tissue, the most widely available clinical material, requires optimized sample-processing strategies to ensure reliable protein extraction and mass-spectrometry analysis. This challenge motivated the work presented in this thesis.

A meningioma is a tumor that grows from the membranes that surround the brain and spinal cord, called the meninges, the outer three layers of tissue between the skull and the brain that cover and protect the brain just under the skull. It is not a brain tumor, but it may press on the nearby brain tissue, nerves and vessels potentially resulting in severe disability or potentially life-threatening complications. In most of the cases meningiomas grow slowly and often without symptoms, which is why it is also very hard to detect in time. It is not known what causes meningioma, however being exposed to radiation as a child is the only known environmental risk factor of developing meningioma. (Mayo Clinic, 2024a)

Overall, meningiomas make up 40.8% of all primary brain tumors in the United States and 56.2% of “nonmalignant” primary brain tumors. Incidence rates of nonmalignant meningioma are the highest amongst all CNS tumors at 9.73 per 100 000 population in the United States. These rates increase after the age of 65 years and again after the age of 85. Age-adjusted incidence rates of nonmalignant

meningiomas continue to increase across different sexes, ethnicities, and races. Meningiomas also account for the largest proportion of intradural spinal tumors in patients 20 years of age and older (39.9%), although spinal meningiomas represent only 4.2% of all diagnosed meningiomas. Nonmalignant meningiomas are 2.3 times more commonly diagnosed in females than in males, and this disparity is the largest between the ages of 35 and 44. Ten-year relative survival for nonmalignant meningioma is 83.4%. (Wang et al., 2024)
The CNS WHO grade 3 or anaplastic meningiomas occur rarely, account for approximately 1%–3% of these tumors and are characterized by aggressive behavior, high recurrence rates, and significant mortality. (Szőke et al., 2025). Data of grade 3 meningiomas show worse outcomes with a 5-year overall survival rate of 66%, and an estimated 10-year overall survival of only 14–24%. (Wang et al., 2024)

The treatment for meningiomas depends on the location in the brain where it grows, rate of growth, age and overall health. A slow growing meningioma might not need a treatment right away, instead it can be observed by professionals over time. If then it is starting to grow or it is causing symptoms, then surgery might be suggested. With most cases being benign, they are treated with surgery. Radiation therapy is not the first choice of treatment as it is not effective in many patients and can make future surgery more difficult, however it can be used in patients who are too sick for surgeries or when complete resection is impossible. It can also be used if the meningioma is in a high-risk location for surgery. In case of grade 2 meningiomas that could not be completely removed as well as for all grade 3 meningiomas, radiotherapy is the therapy of choice (Goldbrunner et al., 2021). Chemotherapy is almost ineffective for meningiomas, however be tried if surgery and radiotherapy are not an option (Mayo Clinic, 2019). In addition, effective molecular targeted therapies are not known, only some investigational indications are currently accepted (Sahm et al., 2025). Therefore, the identification of novel therapeutic targets and exploration of the complex biological events driving meningioma progression is of great clinical relevance.

Grade 3 meningiomas can appear primarily (“de novo”) or they can result from the transformation of lower grade tumors. Recent multiomic studies provided data that allow for a more precise grading of the tumors than the traditional histopathological way. These studies have also provided insights into the mechanisms of the progression of meningioma as well as the biology of the

aggressive ones. The epigenetic regulator Polycomb repressive complex 2 (PRC2) has been shown to be involved in very aggressive grade 3 meningiomas as well as the progression of meningioma grades. Overexpression of EZH2 (histone methyltransferase enhancer of zeste homolog 2), the catalytic subunit of PRC2, has been associated with increasing meningioma grades and aggressiveness. (Szőke et al., 2025).

This study primarily aims to characterize the proteomic profiles of grade 3 meningiomas in relation to EZH2 expression and other clinical parameters. Another objective is to compare these profiles with those of grade 1 meningiomas in order to identify protein expression differences associated with tumor grade and aggressiveness. In total, 43 FFPE (formalin-fixed, paraffin-embedded) grade 1 and grade 3 meningioma samples were included. Working with FFPE tissue poses two major challenges for proteomic analysis. The first is the efficient removal of paraffin, which is commonly performed using xylene, although less toxic substitutes such as heptane are increasingly used. However, only few studies have examined how these alternative clearing agents affect the protein yield. (Humphries et al., 2024) The other challenge is the inter- and intraprotein crosslinking introduced during the fixation process, which complicates tissue lysis and digestion and often results in low protein/peptide yield. (Humphries et al., 2024) Therefore, another aim of this study was to develop and implement a sample preparation protocol that maximizes protein yield while allowing efficient processing of large samples numbers.

Taking these together, the overall goal of this project was to establish and apply a robust proteomics workflow for FFPE meningioma tissue in order to investigate proteomic differences between grade 1 and grade 3 tumors, explore heterogeneity within high-grade meningiomas, and identify proteomic patterns that correlate with EZH2 expression and relevant clinical variables. To address this aim, the work was divided into two main parts. The first part focused on sample preparation optimization using pilot tissues to test and refine the deparaffinization, lysis, extraction, and digestion steps, with the goal of selecting a protocol suitable for the clinical cohort. The second part applied the optimized workflow to the full set of FFPE meningioma samples, followed by comprehensive proteomic data analysis to compare grade-specific protein expression, assess intra-grade heterogeneity, evaluate associations with clinical and molecular parameters, and compare the performance of the tested preparation methods.

Structure of this report:

The Introduction outlines the clinical and biological background of meningiomas and the motivation for using proteomics. The Methodology chapter describes the experimental workflow, including sample preparation, LC-MS/MS acquisition, and data analysis procedures. The Results and Discussion chapter presents findings from both the pilot optimization and the analysis of the whole cohort, while integrating these findings with current knowledge, addressing methodological considerations, highlighting study limitations, and outlining future directions. Finally, the Conclusion summarizes the main contributions of this work.

Methodology

This study used a multi-step FFPE tissue proteomics workflow that included deparaffinization, tissue lysis and protein extraction, enzymatic digestion, LC-MS/MS analysis, and final computational data processing.
To establish the final protocol for the meningioma cohort, we evaluated whether the previously developed preparation workflow (Kuras et al., 2021) could be improved in terms of protein yield, proteome coverage, throughput, and processing time. For this purpose, we tested different deparaffinization methods (using EnVisison FLEX or heptane/methanol), compared tissue lysis and protein extraction approaches (Bioruptor vs. BeatBox) and digestion strategies (S-Trap vs. magnetic bead–based digestion). The trials were done using FFPE samples from lung, liver, and xenograft tumor tissues.

Deparaffinization

Deparaffinization using EnVision FLEX solution

For deparaffinization, our published protocol (Kuras et al., 2021) was followed. Briefly, EnVision FLEX Target Retrieval Solution High pH (Agilent Dako) was diluted 10 times, and 1 mL was added to each sample tube. The samples were incubated in a Thermomixer for 10 min at 95°C and then centrifuged at 4°C to pellet the tissue. The supernatant and the paraffin was then removed manually. This process was repeated 3 times, or until no visible wax remained. All the supernatant was then removed from the tubes and the samples were ready for the next step.

Deparaffinization with n-heptane/methanol

For the second deparaffinization method, the procedure was adapted from the protocol reported by Humphries (Humphries et al., 2024). In this approach, 510 µL n-heptane was added to the tissues together with 90 µL methanol, the samples were vortexed and then incubated in a Thermomixer at 37°C for 10 min with shaking at 900 rpm. Following centrifugation, the supernatant was removed, and the samples were left to dry for about 5 min or until all solvent had evaporated.

Protein extraction

For both extraction protocols, lysis buffer (4 w/v% SDS, 10 mM DTT in 100 mM TEAB, pH 8.0 or 4 w/v% SDS, 10 mM DTT in 100 mM TRIS-HCl, pH 8.0) was added to the deparaffinized tissue. Mechanical disruption was performed either with the Bioruptor Plus or the BeatBox system, after which all samples were incubated at 95 °C in a Thermomixer for 1 hour with shaking to induce antigen

retrieval and reverse crosslinking. Samples were then centrifuged to clarify the lysates.

Protein extraction using Bioruptor

For the Bioruptor Plus (Diagenode) extraction, 200-300 µL of lysis buffer was added to each tube containing the deparaffinized samples. The tubes were then placed in the Bioruptor Plus and sonicated for 20-40 cycles (15 s on / 15 s off), and briefly centrifuged before the 95°C incubation step. After the 1-hour incubation, the tubes were centrifuged at 15000 g, for 10 min at 22°C, and the supernatants were then placed in new tubes, and 4 µL was taken from for protein determination.

Protein extraction using BeatBox

For the BeatBox (PreOmics) protein extraction, a 96-well plate was used. The dry tissues were loaded into the wells using tweezer, and 50 µL of lysis buffer was added first to help loading of the dry tissues, followed by an additional 150µL of lysis buffer to each sample. The plate was then placed in the instrument and run for 2 x 15 min with high-power setting. After the first 15 minutes, the samples were checked for condensation and then run for another 15 minutes. When the BeatBox process was finished, the plate was centrifuged for 30-60 sec at 500 g. The plate was then placed on a metal rack so that the magnetic beads could stick to the walls. The lysates were then removed and placed back into the tubes where the tissues were initially collected and subjected to incubation at 95°C for 1 hour. After incubation, the tubes were centrifuged for 10 min at 15000 g to remove remaining debris. The clarified supernatants were transferred to new tubes, and 4 µL was taken for protein determination.

Protein determination

After protein extraction, protein determination was performed on all samples using the Pierce 660nm Protein Assay with the Ionic Detergent Compatibility Reagent (Thermo Scientific) according to the manufacturers' instructions.

Protein digestion

For all digestion tests, 24–50 µg of protein per sample was used. After protein quantification, lysates were alkylated by adding iodoacetamide (IAA) to a final concentration of 20 mM and incubating the samples for 30 minutes at room temperature in the dark.

S-Trap digestion

S-Trap micro spin columns (ProtiFi) were used, and digestion was performed according to the already existing protocol (Kuras et al., 2021).

Briefly, samples were acidified with phosphoric acid (final concentration 1.2%) and mixed with S-Trap binding buffer (90% methanol in 100 mM TEAB) at a ratio of 1:6 (lysate : binding buffer). The mixtures were loaded onto the S-Trap columns and centrifuged to capture the proteins. The filters were washed with binding buffer, and digestion was carried out directly on the column by adding trypsin (1:25, w/w, enzyme:protein) in 50 mM TEAB and overnight incubation at 37 °C. Peptides were eluted in three steps (50 mM TEAB, 0.1% formic acid, and 50% acetonitrile/0.1% formic acid) and dried in a centrifugal evaporator.

Manual magnetic bead–based digestion

MagReSyn hydroxyl magnetic beads (ReSyn Biosciences) were used for bead-based digestion following the manufacturer's protocol. Beads were equilibrated and mixed with the protein lysates in the presence of 70% acetonitrile to induce protein binding to the bead surface. After binding, beads were washed with 100% acetonitrile and 70% ethanol to remove detergents and contaminants. On-bead digestion was performed by adding trypsin (1:25, w/w, enzyme:protein) in 50 mM TEAB and incubating the samples overnight at 37 °C. Digestion was stopped by adding TFA to a final concentration of 1%. Supernatants were collected and dried in a centrifugal evaporator.

Automated magnetic bead-based digestion

Magnetic bead-based digestion was also automated on the KingFisher Apex instrument to compare performance with the manual procedure. Two versions of the protocol were tested: with and without bead pre-equilibration. In the pre-equilibration workflow, beads were equilibrated in 70% acetonitrile before being released into the tissue lysate, while in the non-pre-equilibration workflow, beads were added directly to the lysate.

Both workflows followed the same additional steps: three washes with 100% acetonitrile, two washes with 70% ethanol, and on-bead digestion in 50 mM TEAB with trypsin at 47 °C for 2 hours. In this workflow, different enzyme-to-protein ratios as well as both single-enzyme (trypsin) and two-step (LysC followed by trypsin) digestions were evaluated. Peptides were collected and acidified before LC-MS/MS analysis.

nanoLC-MS/MS analysis

Dried peptides were resuspended in 2%ACN with 0.1%TFA to maximize peptide recovery. Samples were analyzed using data-independent acquisition (DIA) on two different LC-MS/MS platforms. A subset of samples was analyzed on an Orbitrap Exploris 480 mass spectrometer (Thermo Scientific) coupled to a Vanquish Neo nano-UPLC system with an EASY-Spray ion source. Approximately 500 ng of peptides per sample was loaded onto an Acclaim PepMap 100 C18 trap column and separated on an Easy-spray PepMap RSLC C18 column (75 µm × 50 cm, 2 µm, 100 A) using a 60-min gradient. DIA data were

acquired using twenty-six variable isolation windows across the 350–1650 m/z range.
Another subset of samples and the whole meningioma cohort were analyzed on a timsTOF HT mass spectrometer (Bruker) coupled to an Evosep One LC system. (Evosep Biosystems) For these analyses, 500 ng of peptides were loaded onto Evotips according to the manufacturer's instructions and separated using the 30 samples-per-day (SPD) gradient on a 15-cm Evosep column packed with 1.5 µm ReproSil-Pur C18-AQ particles. Data were acquired using the factory optimized diaPASEF method, combining trapped ion mobility spectrometry with DIA using predefined ion mobility and m/z windows.

Data processing and bioinformatic analysis

Spectronaut- DIA search

Raw DIA files were analyzed in Spectronaut vs19 (Biognosys AG) using the library-free workflow with default factory settings and MS2-based quantification. Searches were performed against the UniProt human reference proteome (20371 entries). Carbamidomethylation of cysteine was set as a fixed modification, and methionine oxidation was considered as a variable modification. Up to two missed cleavages were allowed. False discovery rate (FDR) control was applied at 1% both the peptide and protein levels.

Data analysis

Peptide-level reports, were analyzed in MATLAB to assess digestion efficiency and in Excel to compare the number of identified/quantified peptides across samples. For the latter, peptides were considered confidently detected if they appeared in at least two out of three replicates for each method or condition. These peptide lists were used to compare overlap between methods or conditions. Venn diagrams showing shared and unique peptides were generated using an online Venn diagram tool, Venny (https://bioinfogp.cnb.csic.es/tools/venny/).
Protein-level quantification tables generated in Spectronaut were imported into Perseus (Tyanova et al., 2016) for processing. Protein intensities were log2-transformed and normalized across samples to reduce experimental variability. To compare the number of proteins identified/quantified across samples and conditions (e.g., different preparation methods, disease groups), a matrix containing only valid values was created by using the "summary statistics (column)" function in Perseus. The number of protein identifications for each sample/condition was then plotted as bar plots and/or Venn diagramms.
For the full meningioma cohort, differential protein abundance between sample groups was assessed using the limma package in R. Log_2-transformed and normalized protein intensities were fitted using linear models with empirical Bayes moderation to improve variance estimates. P-values were adjusted for

multiple testing using the Benjamini–Hochberg method, and proteins with adjusted p-value < 0.05 were used for downstream pathway enrichment analysis. Grade 3 meningioma samples were further clustered to explore intra-grade heterogeneity. Hierarchical clustering was performed using correlation distance and Ward.D2 linkage for proteins (rows), and Euclidean distance with Ward.D2 linkage for samples (columns), based on the top 1000 most variable proteins. After cluster assignment, clinical parameters were compared between the resulting groups using the Mann–Whitney U test for continuous variables and Fisher's exact test for categorical variables. A significance threshold of $p < 0.05$ was applied. Pathway enrichment analysis was performed using the WEB-based GEne SeT AnaLysis Toolkit (https://www.webgestalt.org/; Elizarraras et al., 2024)

Results and Discussion

Pilot Studies

Evaluation and optimization of the FFPE sample preparation workflow

Comparison of deparaffinization methods

The first decision that had to be made was to choose a xylene-free approach for the deparaffinization of the FFPE tissues, as xylene is a highly toxic chemical. One of these approaches is the EnVision method, which is an already established but long protocol, with some uncertainty on whether proteins may be lost during the process due to the nature of the protocol. However, there was also the possibility of testing a new protocol that could result in higher protein yield with a much shorter processing time, which is important when processing large numbers of samples at once.

For this reason, the first pilot study was done to establish an alternative deparaffinization method using n-heptane and methanol, and to compare it to the EnVision one. To study these two deparaffinization methods, FFPE lung, liver and xenograft tumor tissues were used. Bioruptor sonication was applied for protein extractions. Based on the Pierce 660nm Assay, protein concentrations obtained from the EnVision deparaffinization were on average more than 50% higher than those obtained from the n-heptane/methanol method.

Although the EnVision method resulted in higher measured protein concentrations, the lysates were heterogeneous and often contained a visible cloudy solution, which was difficult to handle. This likely led to an overestimation of protein levels in the Pierce 660nm Assay. In contrast, n-heptane/methanol method produced clear lysates with lower variability between tissue types, making it more suitable for large-scale cohort processing. It is worth mentioning that these

deparaffinization methods were tested on different tissue types, and some variability may be due to the biological differences.

Comparison of protein extraction methods

In addition to deparaffinization, an alternative protein extraction method, the BeatBox, was also tested on different tissues. The BeatBox method allows the extraction of proteins from a larger number of samples at the same time and in a shorter time than the Bioruptor. The results are summarized in the table below.

Table 1: Protein concentrations obtained using different extraction methods (Pierce 660nm Assay)

	Bioruptor-TEAB (µg/mL)	Bioruptor-TRIS (µg/mL)	Beatbox-TEAB (µg/mL)	Beatbox-TRIS (µg/mL)
Liver		2363		2858
Tonsil	7772	6265	7651	5671
Tumor	1514	2253	1304	1750

To compare the two protein extraction methods fairly, only tissues processed with n-heptane/methanol deparaffinization were used, as EnVision-treated tissues were very challenging to handle with the BeatBox. As can be seen from the table, BeatBox and Bioruptor yielded comparable protein concentrations across the different tissues, with differences of ≤10–15% for most samples. BeatBox showed lower variability for tonsil samples and offered significantly higher throughput, supporting its selection for the final workflow. Also considering the advantages mentioned previously, it was the best choice for the final protocol. To confirm this choice, the different extraction methods was further verified in the following tests.

Comparison of complete sample preparation workflows including digestion

After evaluating the initial results, further testing was done on FFPE tonsil samples using the two deparaffinization methods and the two protein extraction methods, followed by protein determination using the Pierce 660nm Protein Assay. The aim with this trial was also to test two different digestion methods, including S-Trap-based digestion and magnetic bead-based (MagReSyn) digestion.

For clarity, the three tissue-processing combinations used in this comparison are defined as follows:

A: EnVision deparaffinization + Bioruptor extraction

B: n-heptane/methanol deparaffinization + Bioruptor extraction

C: n-heptane/methanol deparaffinization + BeatBox extraction

These three combinations (A–C) were tested with the two digestion methods (S-Trap and MagReSyn).

Prior to protein digestions, the appropriate lysis buffers were prepared for each workflow. For the S-trap digestion a lysis buffer consisting of 4 % SDS in 100mM

TEAB (pH 8.0) with 10mM DTT was used. For the magnetic bead-based digestion the lysis buffer consisted of 4% SDS, 10mM DTT in 100mM TRIS (pH 8.0). The results from these tests are presented below.

The following figures (Figures 1-6) present the results from the different tissue processing workflows, allowing the comparison of the different methods and selection of the most suitable one for processing of the real meningioma samples.

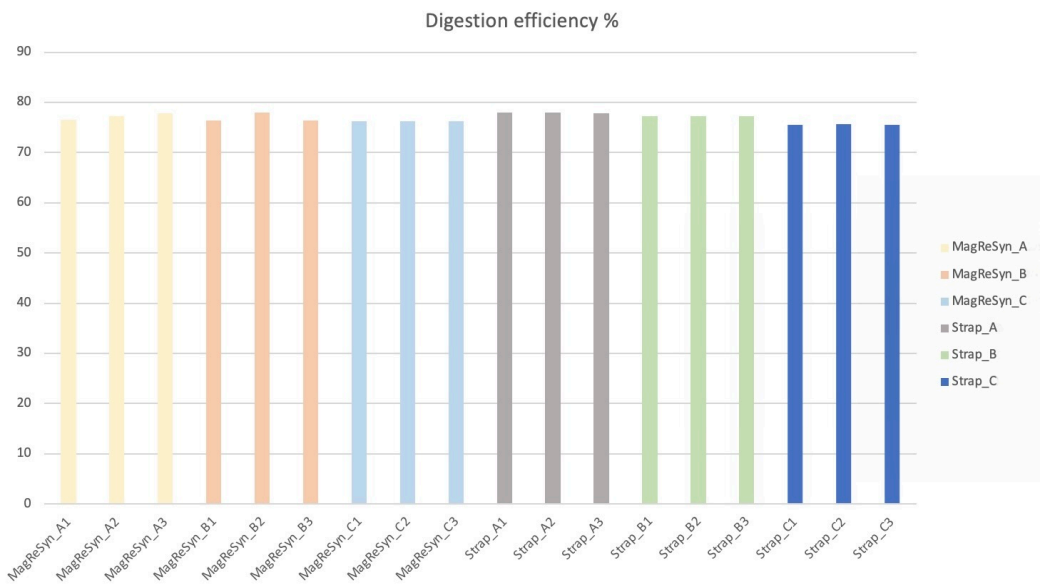

Figure 1. Digestion efficiency obtained from the different sample processing workflows. Digestion efficiency (%) represents the proportion of fully cleaved tryptic peptides in each sample. The letters, A, B and C represent the different combinations of tissue processing steps, used prior to digestion. A: EnVision + Bioruptor, B: n-heptane/methanol + Bioruptor, and C: n-heptane/methanol + BeatBox. The numbers indicate replicates in each method.

The digestion efficiency is presented in Figure 1 for the two different digestion methods (MagReSyn and the S-Trap) across the different processing protocol combinations. Overall, there were no major differences in digestion efficiencies between the different methods. To be able to decide which method would be most suitable, further analyses were done by evaluating the number of identified proteins and peptides, as well as the overlap between methods.

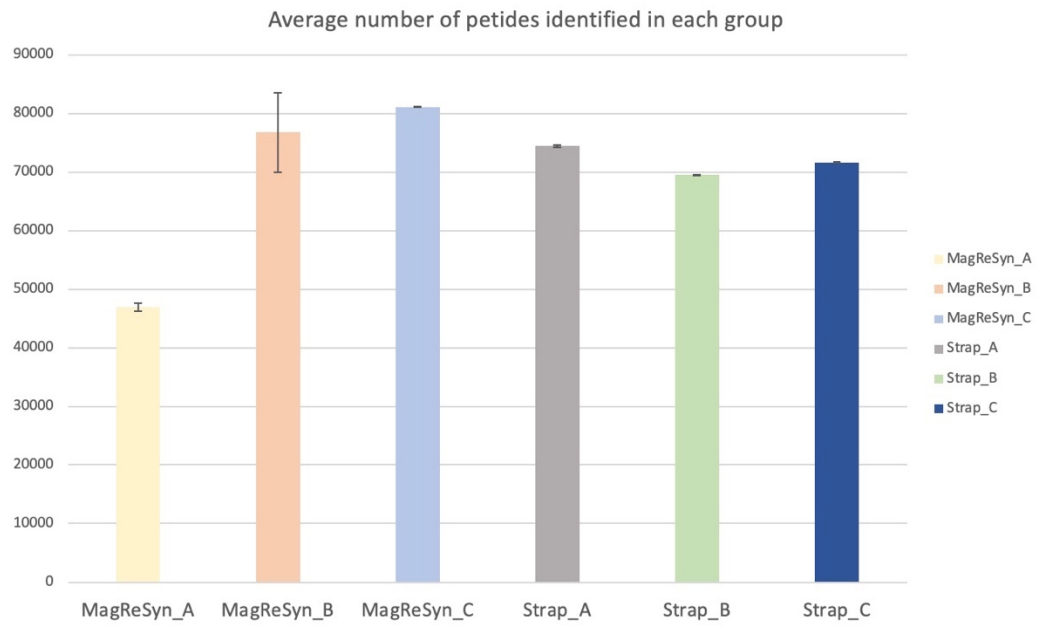

Figure 2. The average number of identified peptides in each sample processing method

From Figure 2, it is clear that the magnetic bead-based digestion in combination with the n-heptane/methanol + BeatBox workflow (C) resulted in the most identified peptides compared to the other methods, as well as the best reproducibility.

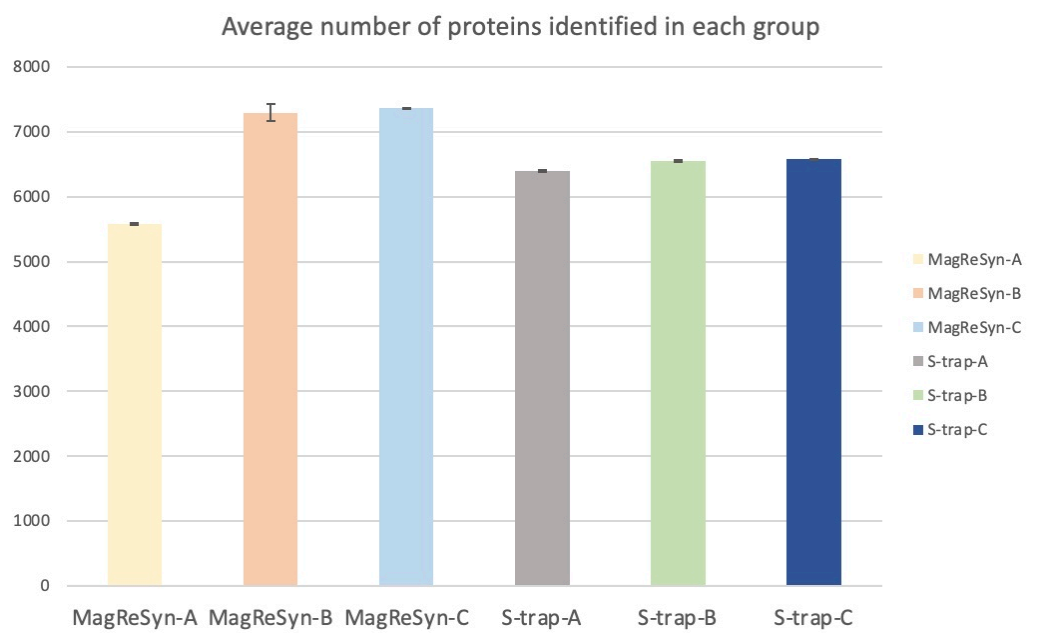

Figure 3. The average number of proteins identified in each sample processing method

The comparison of protein identifications clearly demonstrated that magnetic bead-based digestion provides better results than S-Trap. An evident outlier in Figure 2 and Figure 3 was the EnVision + Bioruptor tissue processing with magnetic bead-based digestion. The results from the EnVision processed tissues were the least reliable due to the most challenging to handle (cloudy) lysates. This again supports the choice of the n-heptane/methanol deparaffinization, which was also quicker and less complicated.
The best protein identifications were observed from magnetic bead-based digestion, when it was combined with n-heptane/methanol + BeatBox tissue processing (MagReSyn-C in Figure 3). These results are consistent with the results from Figure 2.

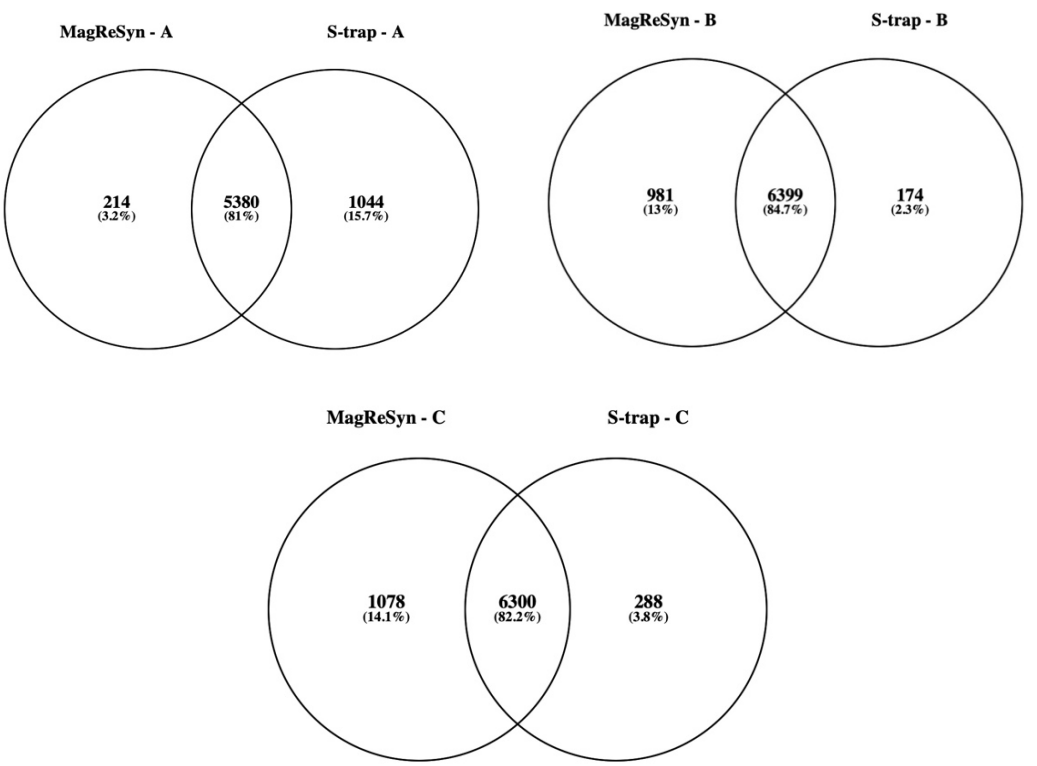

Figure 4. Protein overlap between MagReSyn and S-Trap digestion using the three tissue-processing methods A-C.

Venn diagram analysis revealed that >80% of proteins were shared between the two digestion methods, but MagReSyn digestion consistently contributed a substantial number of unique identifications (Figure 4). The opposite could be

seen only in method A, where S-Trap digestion resulted in more uniquely identified proteins (Figure 4). This is likely due to the difficulties in handling the lysates that have undergone EnVision deparaffinization. Those lysates were often cloudy and it was challenging to transfer them reproducibly from one tube to another, as well as to measure their protein concentration in a reproducible way.

Based on the combined evaluation of digestion efficiencies with the number of identified peptides and proteins, magnetic bead-based digestion was selected for the final protocol in combination with n-heptane/methanol deparaffinization and BeatBox protein extraction.

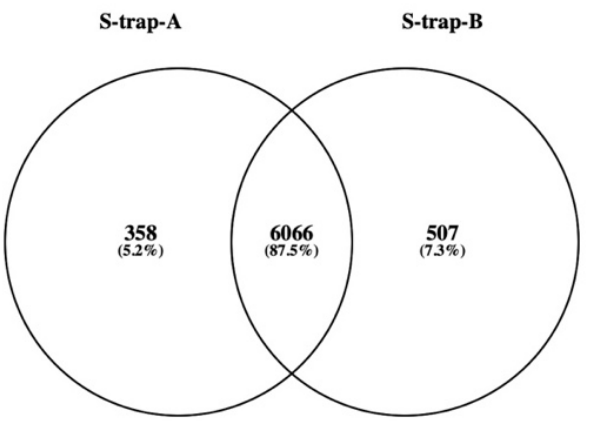

Figure 5. Protein overlap between the EnVision vs n-heptane/methanol depparaffinization methods.

To further validate the choice of deparaffinization method, the overlap between S-Trap-A and S-Trap-B was investigated (Figure 5). The two conditions shared 87.5% of the proteins, however S-trap-B (n-heptane/methanol deparaffinization) had a higher protein identification number than the EnVision one, which supports the choice of the n-heptane/methanol method.

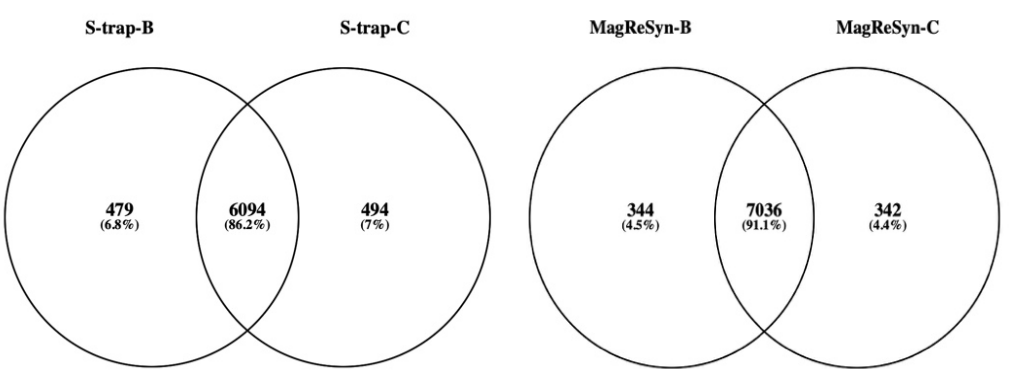

Figure 6. Protein overlap between Bioruptor vs BeatBox protein extractions combined with S-Trap (A) and MagReSyn (B) digestion.

Because digestion strategy can influence peptide and protein identifications, overlap between the two protein extraction approaches was evaluated separately for the S-Trap and MagReSyn workflows. In both digestion methods, a large proportion of proteins was shared between the two conditions. In the S-Trap digestion, the Beatbox extraction showed a slightly larger set of identifications, while it was almost the same in the MagReSyn digestion (Figure 6). These Venn diagrams reinforce the previous results and support BeatBox as the preferred protein extraction method.

Automated magnetic bead-based digestion using KingFisher Apex

To evaluate whether magnetic bead–based digestion could be automated without compromising performance, tonsil tissues were digested using three workflows, manual magnetic bead-based digestion, KingFisher digestion with bead pre-equilibration (preEQ), and KingFisher digestion without pre-equilibration (no-preEQ). The digestion time is much shorter with this method and the procedure is more automatized than the previous magnetic bead-based protocol which is completely manual and more time consuming. At the same time a more automatized method, means less variation between the processing of each sample. Given the big number of samples that had to be digested for the real meningioma samples, it would be very useful if this method would have similar results in terms of protein and peptide counts compared to the manual protocol.

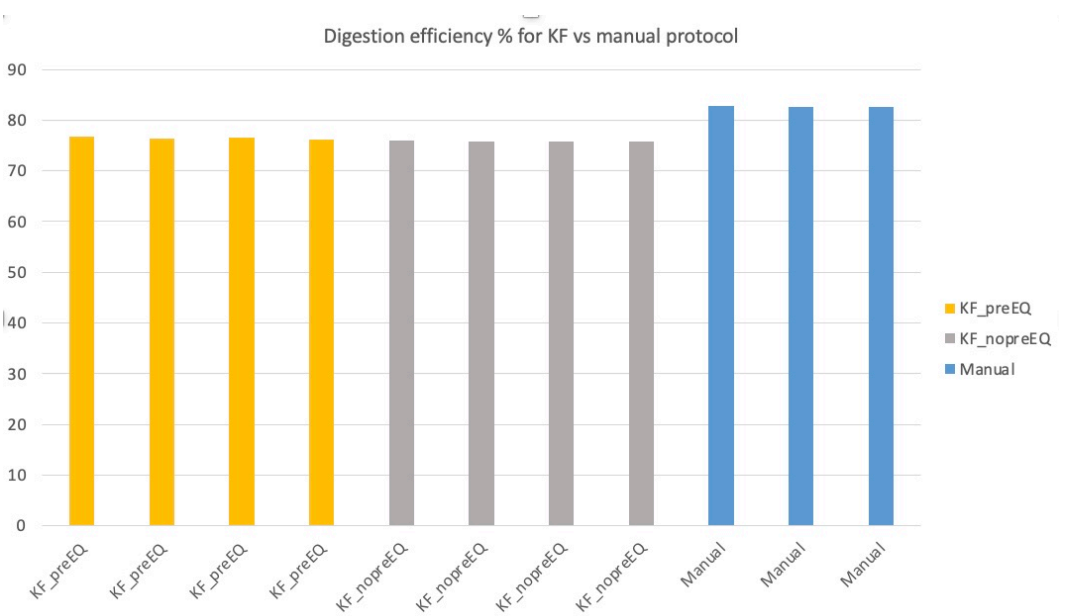

Figure 7. Digestion efficiencies obtained from the KingFisher digestion, with pre-equilibration vs no pre-equilibration and the manual digestion.

In Figure 7, the digestion efficiencies for each method are presented. It can be noted that the manual digestion resulted in better digestion efficiency, however that could be due to the overnight digestion in the manual protocol, which allows more time for cleavages. The KingFisher workflow, on the other hand, is completed in less than 3 hours. There was no significant difference between the pre-equilibration or no pre-equilibration conditions in the KingFisher digestion protocol.
More analysis of peptide and protein identifications was needed to be able to decide whether the manual or the automated KingFisher protocol would be more convenient.

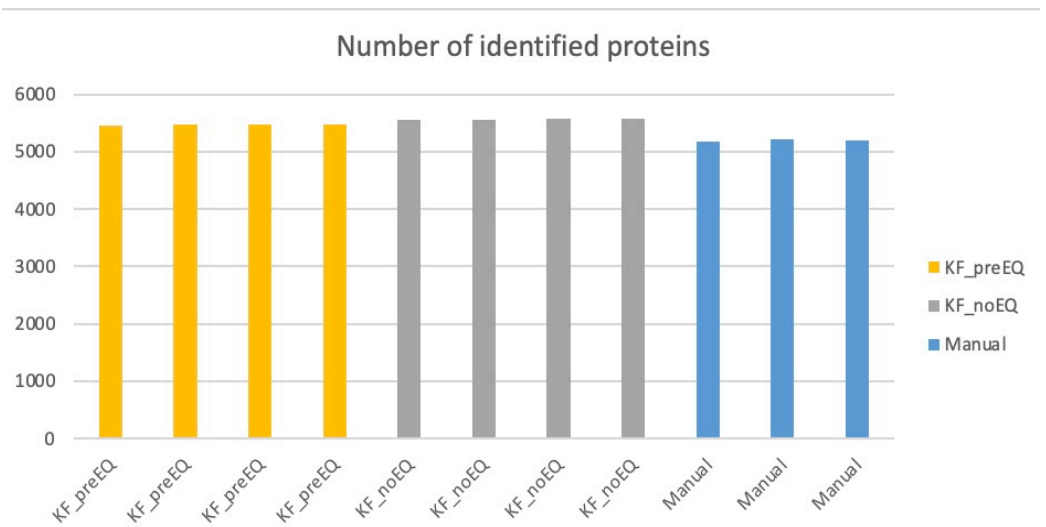

Figure 8. The number of proteins identified in each sample digestion method.

Even though the manual protocol resulted in the highest digestion efficiency, the protein identifications were significantly lower. The bar chart in Figure 8 also shows that the KingFisher workflow without the pre-equilibrating step has resulted in the highest protein identifications.

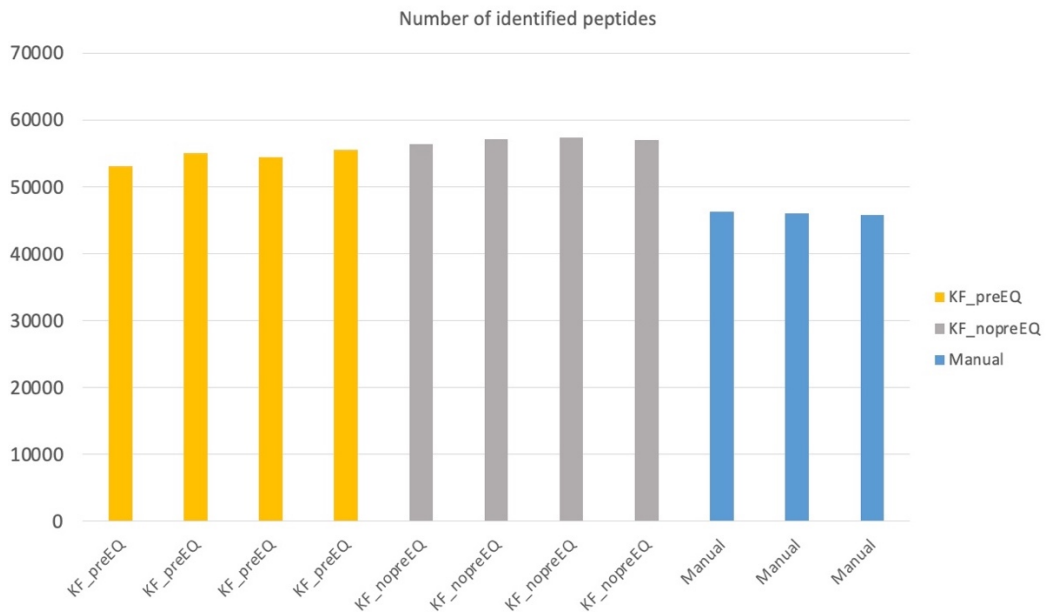

Figure 9. The number of peptides identified in each sample digestion method

The peptide identification numbers confirmed the results from the protein identifications. The same trend can be observed in this figure (Figure 9) across all conditions. Although, the manual protocol showed slightly lower peptide and protein counts than the KingFisher protocols, the difference was less drastic for proteins than for peptide identifications. Based on these results, the KingFisher workflow was selected as the preferred digestion method.

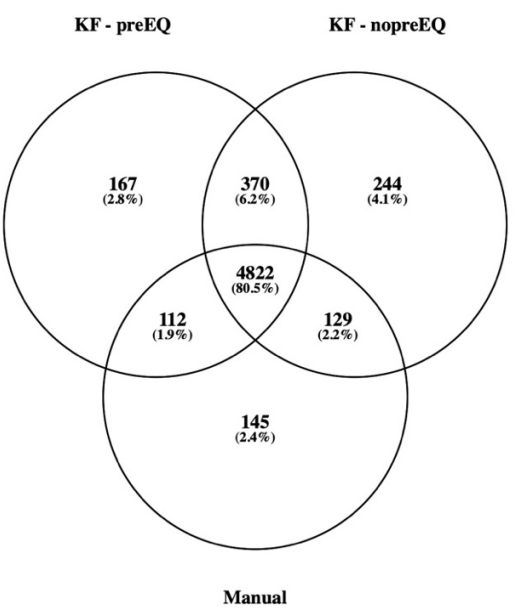

Figure 10. Protein overlap between KingFisher with pre-equilibration, KingFisher without pre-equilibration and manual digestion.

The Venn diagram showing protein overlap (Figure 10), reaffirms that the KingFisher protocol covers the largest protein set, sharing 80,5% of proteins with the other conditions, however KingFisher has the highest identification of unique proteins. It has to be noted that the KingFisher protocol without the pre-equilibrating step has the highest number of unique protein identifications, being 244.

KingFisher digestion on meningioma samples (preEQ vs no-preEQ)

Further testing was done to investigate whether including a pre-equilibration step would result in better protein digestion. For both conditions, two different protein loading amounts (25µg and 50µg) were used. Only the 50 µg protein input was included in the presented results, as pilot experiments demonstrated high variability in the number of identified peptides and proteins when only 25 µg was loaded. Using 50 µg reduced this variability and maximized protein and peptide identifications. Furthermore, two types of digestions were tested, trypsin alone and trypsin-lysC combined digestion, to see which protocol would give better identifications.

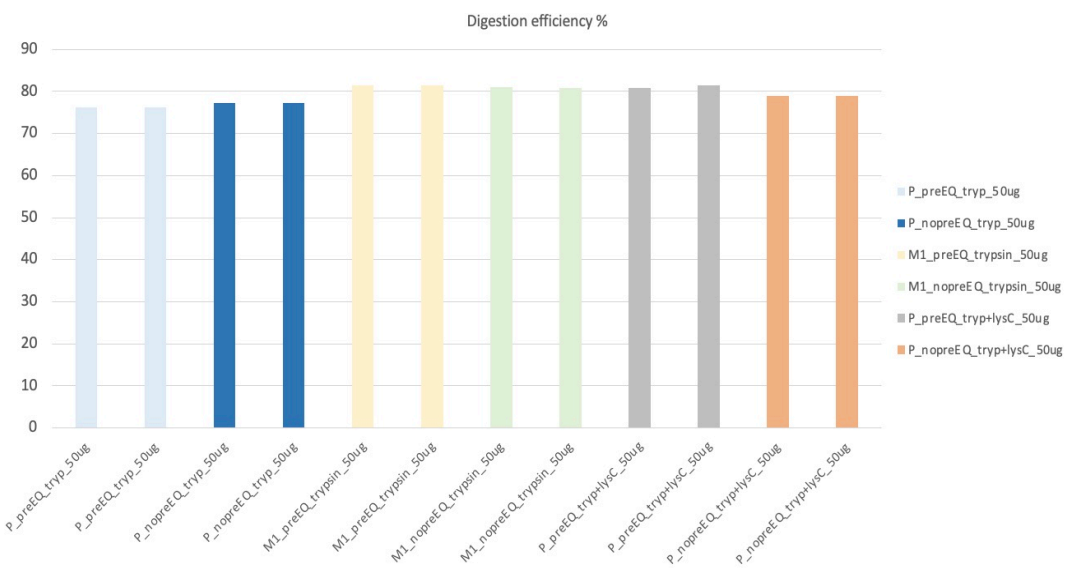

Figure 11. Digestion efficiencies obtained from the KingFisher digestion, with pre-equilibration vs no pre-equilibration and trypsin vs trypsin+lysC.

Figure 11 presents the digestion efficiency results. The digestion efficiency was very similar in both pre-equilibrated and no pre-equilibrated conditions for all enzyme combinations, indicating that the addition of the pre-equilibration step does not have a significant effect on digestion efficiency. The 50 µg protein load

was less affected by pre- vs no pre-equilibration, giving more consistent results. The combined trypsin+ lysC enzyme digestion showed slightly better results in the pre-equilibration condition.

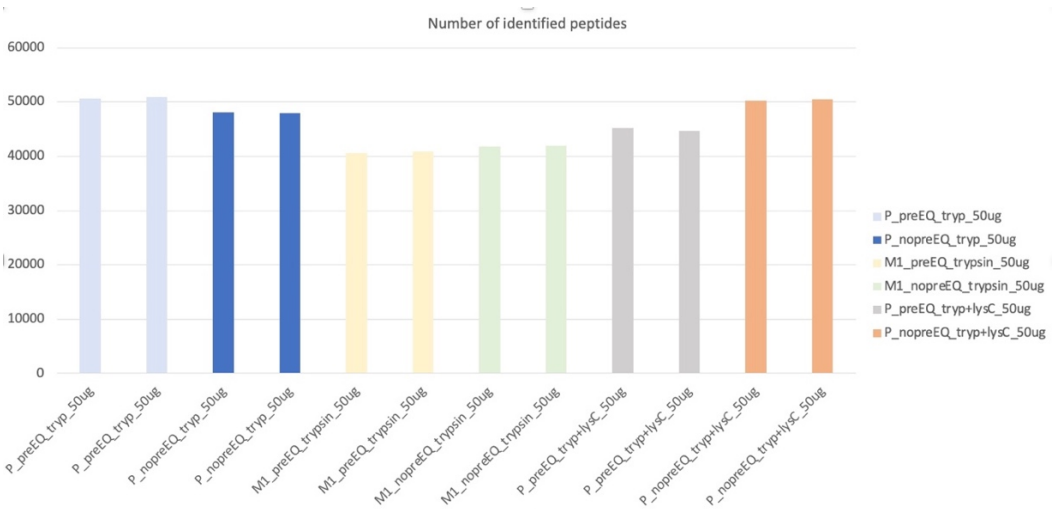

Figure 12. The number of identified peptides in each sample processing method.

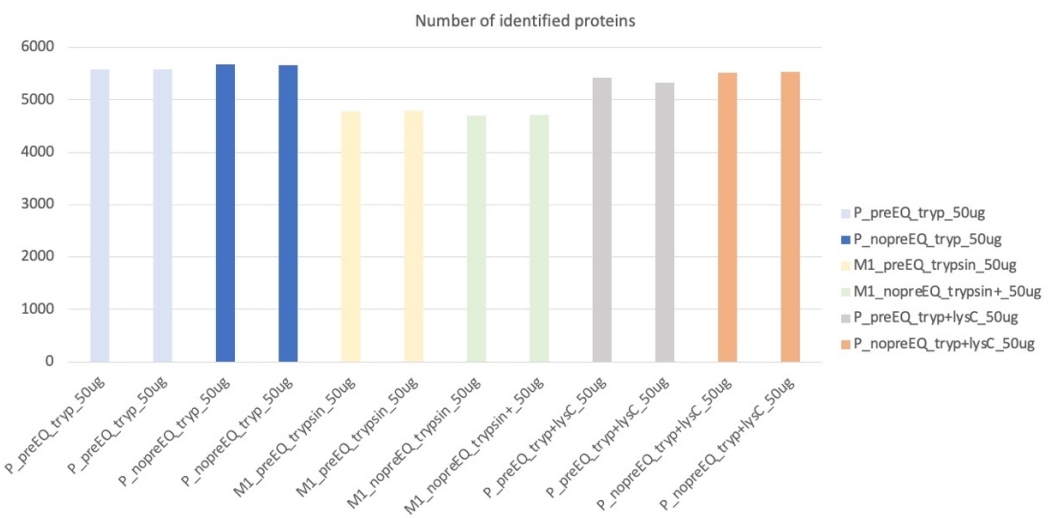

Figure 13. The number of identified proteins in each sample processing method.

The results from protein identification generally follow the trend of the peptide results for each sample (Figures 12-13). Across the pooled meningioma samples, the no-preEQ workflow mostly yielded a higher number of identified peptides and proteins compared to preEQ. This trend was more pronounced when trypsin and LysC were applied together. The combined enzymatic digestion improved cleavage efficiency, which was reflected by slightly increased protein and peptide

identifications Notably, this dual-enzyme approach did not increase processing time and was therefore included in the final protocol.
For 50 µg samples, the no-preEQ workflow produced generally the highest peptide and protein identifications, outperforming both the pre-equilibrated and manual digestions. Although digestion efficiency was slightly lower than in manual digestion, the peptide and protein identifications, as well as reproducibility were superior. Adding LysC together with trypsin increased digestion efficiency and improved identification of larger proteins, supporting its inclusion in the final protocol.

Analysis of the meningioma cohort

The final protocol used to process the 43 meningioma samples consisted of an n-heptane/methanol deparaffinization, followed by protein extraction using the BeatBox instrument, and a one-hour boiling step to induce antigen retrieval. Protein determination was done by the Pierce 660nm Assay. Digestion was then performed using the KingFisher Apex system without the pre-equilibration step, loading 50µg of proteins per sample, and using trypsin with lysC for a more efficient protein cleavage.
Before performing biological comparisons, quality control (QC) assessment was done to evaluate data quality and potential sample outliers. Protein identifications were compared across samples, and pooled QC samples were also monitored.

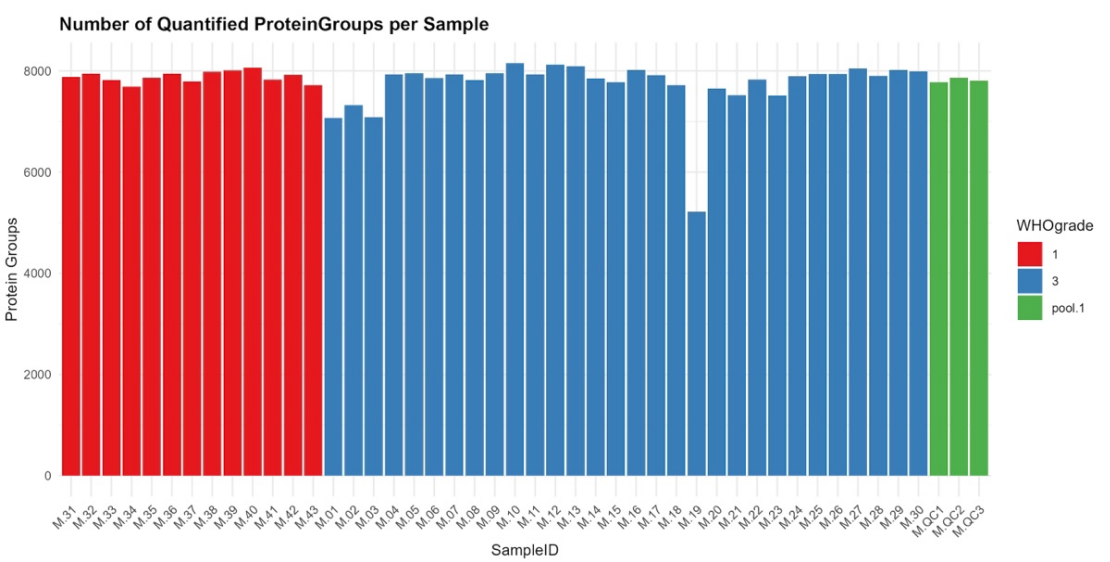

Figure 14. Number of protein IDs per sample. The samples are grouped according to tumor grade, with grade 1 shown in red, grade 3 in blue, and pooled QC samples in green.

Overall, protein quantification and recovery appeared consistent across the cohort. Figure 14 presents the number of identified proteins in each sample. Most samples showed similar protein identifications. However, one clear outlier could be observed (sample 19), which showed considerably lower protein identifications than the rest.

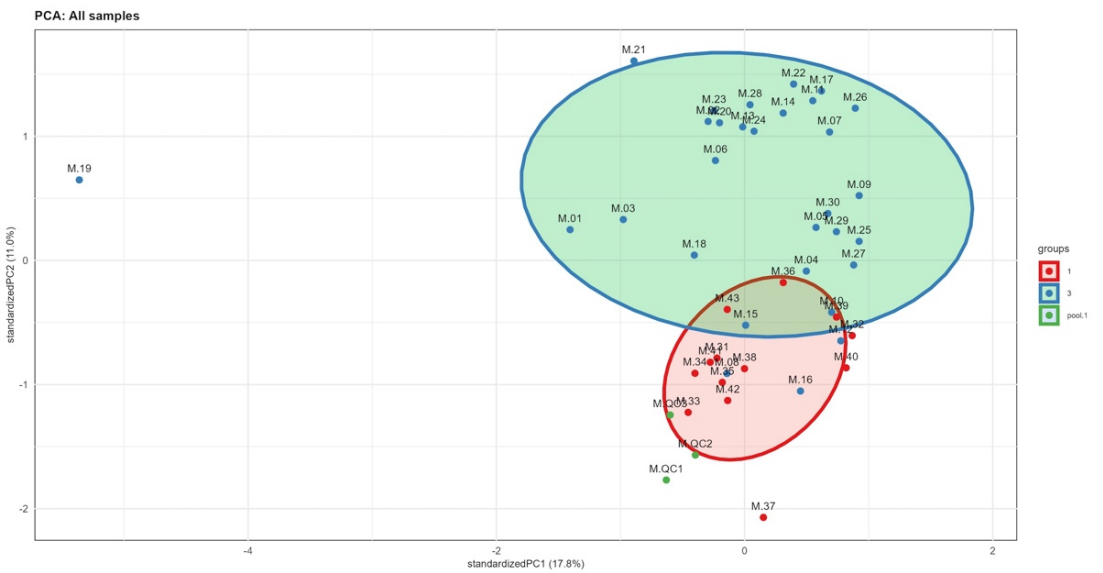

Figure 15. PCA plot of all samples

The PCA plot in Figure 15 shows a partial separation between grade 1 and grade 3 meningiomas. This separation is not perfect, as there is some overlap between the two groups, which might be due to shared biological features of the tumors. Grade 3 meningiomas display a broader spread, which could be explained by a higher proteomic heterogeneity. In contrast, grade 1 meningiomas cluster more closely together, which reflects a more homogenous proteomic profile. Importantly, the pooled QC samples (green) cluster very close together, demonstrating good reproducibility of the processing workflow. It is also worth mentioning that the QC samples originate exclusively from grade 1 meningiomas, and they cluster closely with the individual grade 1 tumors, further supporting the robustness of the data. The PCA plot also confirms sample 19 as an outlier, and it was therefore excluded from further analyses.

Proteomic differences between high-grade (grade 3) and low-grade (grade 1) meningiomas

The proteomic analysis of the meningioma cohort continued with a direct comparison of grade 3 and grade 1 meningiomas to investigate proteomic profiles associated with tumor aggressiveness. As already indicated by the PCA results (Figure 15), tumor grade seems to be an important source of proteomic variation, although some overlap remains between the groups. Our analyses therefore focused on identifying significantly different proteins and exploring the biological pathways they represent.

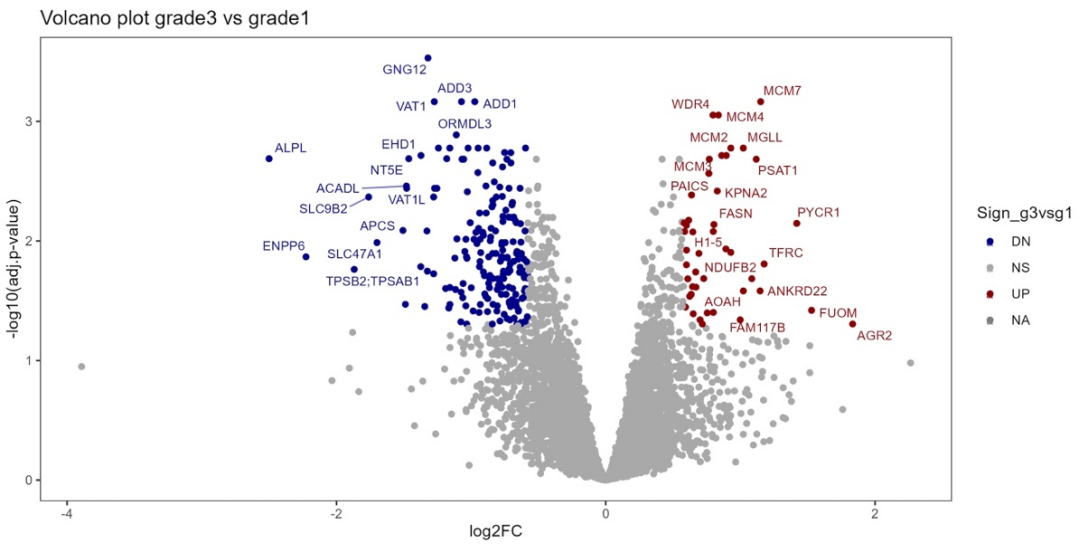

Figure 16. Volcano plot showing differential protein expression between grade 3 and grade 1 meningiomas. Proteins upregulated in grade 3 are shown on the right, with the most significant highlighted in red. Proteins upregulated in grade 1 are shown on the left, with the most significant highlighted in blue. The significance threshold was adjusted p-value < 0.05.

Differential expression analysis was performed using limma. The results are summarized in the volcano plot (Figure 16). Proteins on the right side of the plot are overexpressed in grade 3 tumors. The ones colored in red are the most significant proteins with the highest fold changes. In contrary, proteins on the left side of the plot are the overexpressed in grade 1 tumors, with blue dots indicating the most significant ones. It is noteworthy to look at the upregulated proteins in grade 3 tumors (red). These proteins include MCM2, MCM4 and MCM7, which are all involved in the process of DNA replication and cell-cycle regulation, supporting the highly proliferative nature of grade 3 meningiomas. Other upregulated proteins, such as FASN, PSAT1, PYCR1, are on the other hand involved in metabolic pathways and indicate metabolic reprogramming commonly seen in aggressive tumors.

What is interesting from these results is the potential connection between PSAT1, a key enzyme in the serine biosynthesis pathway (SBP), and EZH2 activity. The SBP produces methyl donors required for EZH2 to perform H3K27me3 methylation. In some cancers, this process represses the expression of certain microRNAs, which leads to an increase of MYC oncogene activity, and consequently increases EZH2 expression. In addition, MYC promotes the transcription of PSAT1. So they are connected through this feed-forward loop that supports the survival and proliferation of the cancer cells. (Białopiotrowicz et al., 2020)

AGR2 is another upregulated protein in grade 3 meningiomas, which is located in the endoplasmic reticulum (ER) and involved in protein folding, tissue development and regeneration. Its overexpression has been associated with increased tumor growth, metastases, and invasive phenotypes, which can contribute to the aggressive behavior of grade 3 meningiomas. (Salu and Reindl, 2025)

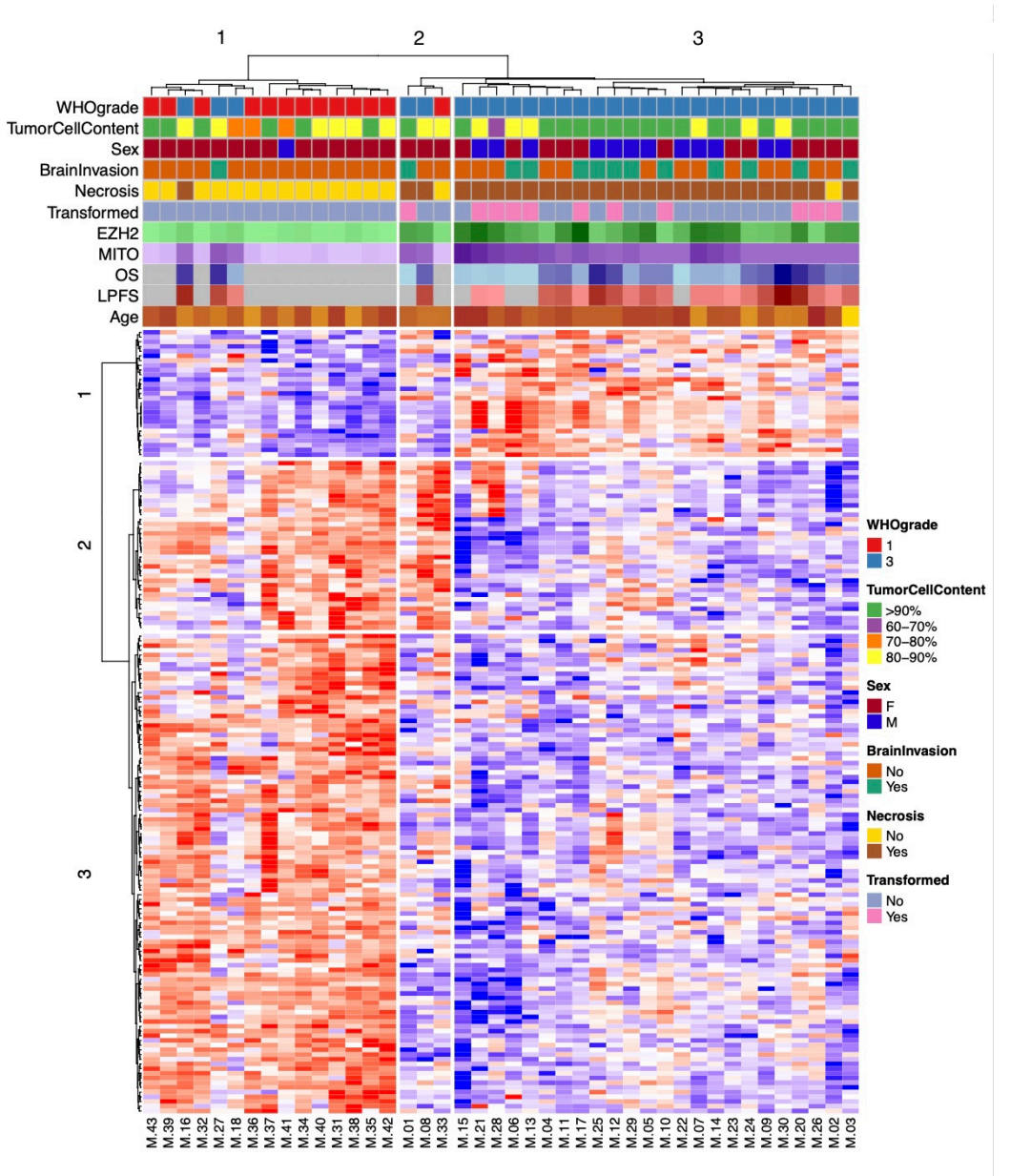

Figure 17. Heatmap of significantly different proteins between grade 3 and grade 1 meningiomas. Samples (columns) and proteins (rows) are hierarchically clustered (Ward.D2; Euclidean distance for samples, correlation distance for proteins). Red indicates higher and blue lower protein abundance.

The heatmap in Figure 17 visualizes the significantly different proteins between grade 3 and grade 1 meningiomas. Each column represents an individual sample, which are hierarchically clustered and grouped mainly into two major clusters corresponding to grade 1 and grade 3 tumors. Even though the separation is not perfect, it can be seen that most grade 3 meningiomas cluster together, and grade 1 tumors form a separate cluster, with only a few samples overlapping. This indicates that tumor grade is a primary source of proteomic differences. Three major protein clusters (numbered as 1-3) can be observed, with proteins belonging to the same cluster showing similar expression patterns across tumors. Proteins in cluster 1 have higher abundance in grade 3 and lower in grade 1 tumors, while proteins in cluster 2 and 3 have generally higher abundance in grade 1 and lower in grade 3 tumors. Proteins in cluster 1 likely reflect more aggressive behavior, including increased proliferation and altered metabolism, which are typical features of high-grade meningiomas.
A few grade 3 tumors cluster closer to grade 1 samples. These tumors also show slightly lower EZH2 expression and lower mitotic index scores compared to the rest of the grade 3 group, suggesting that not all grade 3 tumors display equally aggressive proteomic profiles. This further supports the biological heterogeneity observed within grade 3 meningiomas.
It is also important to note that EZH2 expression is generally higher in grade 3 meningiomas, which is consistent with previous studies where higher EZH2 expression was linked to more aggressive tumor behavior and proliferation. EZH2 expression pattern partially aligns with the mitotic indexes (MITO), which is expected given the higher proliferative activity in high-grade tumors.

These results indicate clear proteomic differences between grade 1 and grade 3 meningiomas, while also highlighting heterogeneity within the high-grade group. To better understand the biological relevance of these differences, pathway-level analyses were performed, including overrepresentation and gene set enrichment analyses (ORA, GSEA).

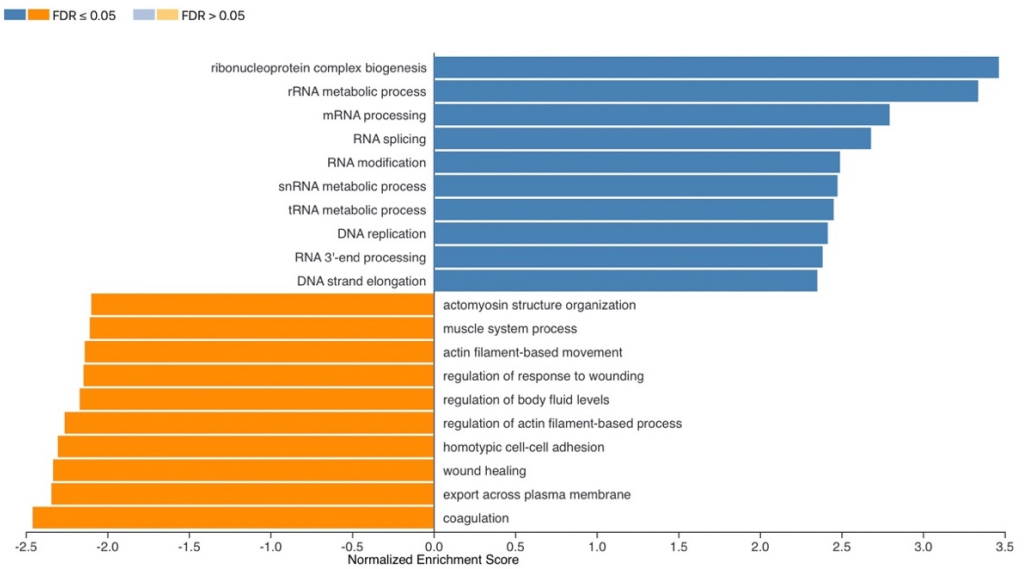

Figure 18. GSEA of grade 3 vs grade 1 meningiomas. Blue bars show the top 10 pathways enriched in grade 3 tumors; orange bars show top 10 pathways enriched in grade 1 tumors.

Figure 18 shows the top enriched pathways for grade 3 vs grade 1 meningiomas based on GSEA. The analysis was performed in WebGestalt using all protein IDs ranked by t-value from the limma analysis. The blue bars represent the enriched gene sets/pathways in grade 3 tumors, where the magnitude of the bar corresponds to the Normalized Enrichment Score. This analysis shows that grade 3 meningiomas are dominated by pathways related to DNA and RNA metabolism as well as proliferation. The most enriched gene sets include RNA metabolic processes, modification and splicing, DNA replication and strand elongations, which are all indicators of highly proliferative tumors. Many of the upregulated proteins in grade 3 from the volcano plot presented above also found in these pathways, which reinforces results. The orange bars, which are the most enriched gene sets in grade 1 tumors provide insights of the nature of grade 1 meningiomas. The dominant gene sets in grade 1 samples are mainly related to cytoskeletal organization, homeostasis and cell adhesion, including coagulation, wound healing, export across plasma membrane gene sets, reflecting a less aggressive biological phenotype.

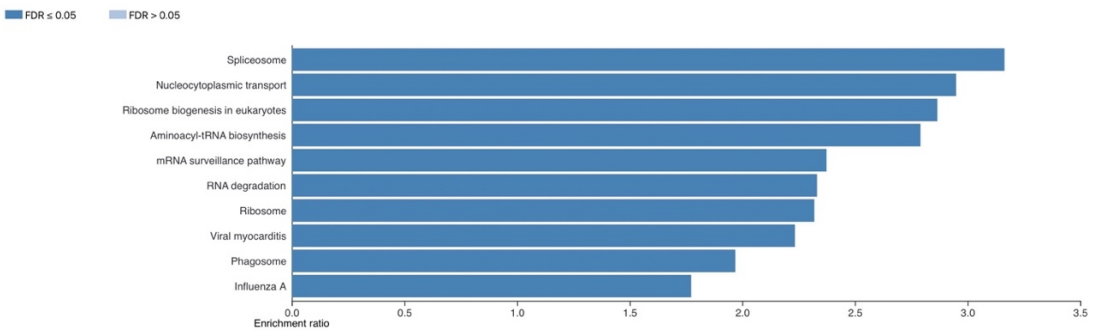

Figure 19. Overrepresentation analysis (ORA) of proteins upregulated in grade 3 meningiomas showing top 10 significantly enriched KEGG pathways.

The bar chart in Figure 19 presents the most significantly enriched pathways in grade 3 meningiomas as compared to grade 1 based on over-representation analysis (ORA) in WebGestalt using the KEGG pathway database. For this analysis, only proteins with positive log2 fold changes (i.e., higher in grade 3) were included. The identified pathways mainly reflect proliferative signaling, nucleic acid metabolism, and other functions typically associated with more aggressive tumor biology, supporting the findings from both the volcano plot and GSEA analyses.

Proteomic differences between high-grade (grade 3) meningiomas.

After comparing proteomic profiles of grade 3 vs grade 1 meningiomas, a further investigation was performed only within grade 3 tumors to explore heterogeneity within high-grade meningiomas and to investigate whether distinct proteomic patterns correlate with EZH2 expression and relevant clinical variables.

Proteomic clustering was first performed using the 1000 most variable proteins across grade 3 tumors, applying hierarchical clustering to group tumors with similar expression profiles. This analysis suggested the presence of three major grade 3 tumor subgroups. These subgroups were then evaluated for their association with clinical and molecular features and further explored by differential expression and pathway analyses.

Table 2: Clinical variables of grade 3 meningioma samples

SampleID	Sex	EZH2 Hscore	Mitoses per mm^2	Transformed	OS time (months)
M.01	F	138,18	14,74	Yes	1,55
M.02	F	140,11	12,63	Yes	37,87
M.03	F	144,91	12,63	No	41,65
M.04	F	64,02	16,84	No	41,91
M.05	M	210,99	12,63	No	36,06
M.06	F	126,29	17,69	Yes	1,81
M.07	M	219,28	20,63	No	16,77
M.08	F	124,55	13,48	No	51,38
M.09	M	71,81	12,63	No	51,87
M.10	F	45,18	12,63	Yes	35,77
M.11	F	173,32	14,32	No	45,79
M.12	M	100,22	13,05	Yes	61,47
M.13	M	109,91	18,11	Yes	1,68
M.14	M	203,40	18,53	No	16,17
M.15	F	202,54	24,85	No	7,17
M.16	F	51,69	12,63	No	69,20
M.17	F	275,20	16,84	Yes	16,14
M.18	F	44,06	12,63	No	15,52
M.20	F	184,51	12,63	Yes	76,73
M.21	M	247,26	22,32	Yes	5,03

M.22	M	103,44	12,63	No	1,05
M.23	F	186,49	16	No	11,31
M.24	F	69,63	12,63	No	44,67
M.25	M	60,73	14,32	No	78,90
M.26	F	45,94	12,63	Yes	57,40
M.27	F	28,14	15,58	No	73,50
M.28	M	194,78	19,37	Yes	6,38
M.29	M	156,12	15,16	No	18,80
M.30	M	91,36	12,63	No	91,52

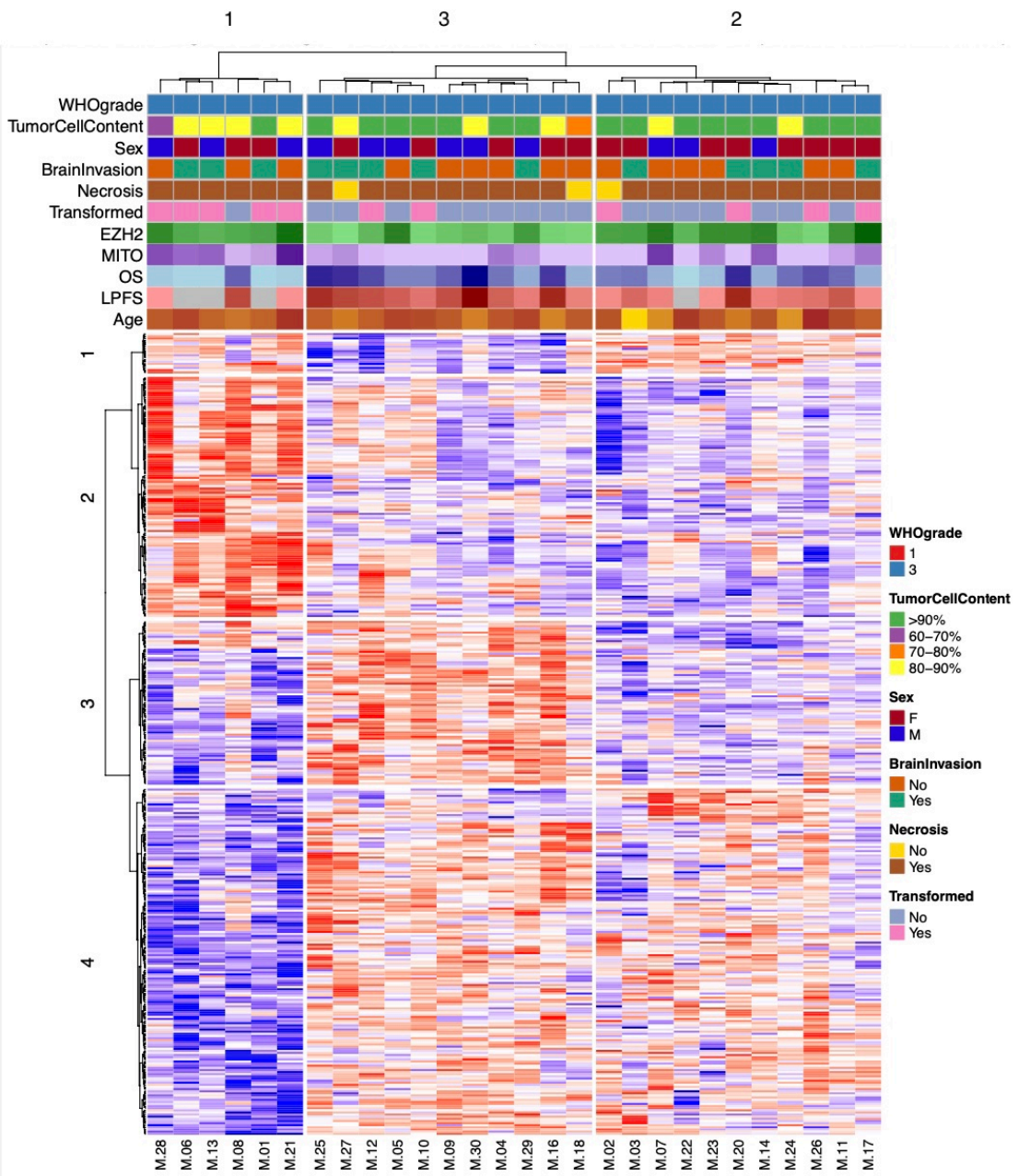

Figure 20. Heatmap of proteomic clusters within grade 3 meningiomas

Figure 20 shows the proteomic clusters within grade 3 meningiomas based on the set of significantly different proteins. Three grade 3 meningioma subgroups (sample clusters) and four protein clusters can be observed. It can be noticed that tumor cell content and sex are distributed across all clusters, suggesting that the

clustering is not driven by these two variables but rather by biological differences. Brain invasion shows some local enrichments but remains spread across the clusters. Necrosis also shows even distribution, however all samples in the first sample cluster are necrosis-positive, whereas the other clusters contain some non-necrotic tumors. Transformation from a lower-grade meningioma shows significant differences between the clusters, with cluster 1 containing a higher proportion of transformed high-grade tumors.

The EZH2 score varies across samples, and it is again interesting to notice that higher mitotic index tends to align with higher EZH2 expressions, which indicates a possible link between EZH2 and proliferative activity. Figure 21 shows that EZH2 scores are the lowest in cluster 3, while mitotic indexes are clearly the highest in cluster 1 compared to the other clusters. Based on EZH2 score, cluster 3 has lowest score indicating a less aggressive tumor, while it is highest in cluster 2 and slightly lower in cluster 1. Mitosis index indicates the number of cells that are proliferating hence indicating a more aggressive tumor. It can be seen that as cluster 1 has a high EZH2 score it also has the highest mitotic count and the worst survival time with just a few months. This indicates highly aggressive tumors compare to the other clusters. Cluster 3 on the other hand displays the lowest EZH2 score, mitotic count and highest overall survival time, indicating the least aggressive tumors out of the 3 clusters.
In terms of clinical outcome, overall survival (OS) differs between the three proteomic clusters, cluster 1 shows the poorest prognosis, whereas cluster 3 demonstrates the most favorable survival, with cluster 2 displaying an intermediate outcome. These patterns suggest that the three proteomic clusters reflect biologically meaningful subgroups within grade 3 meningiomas.

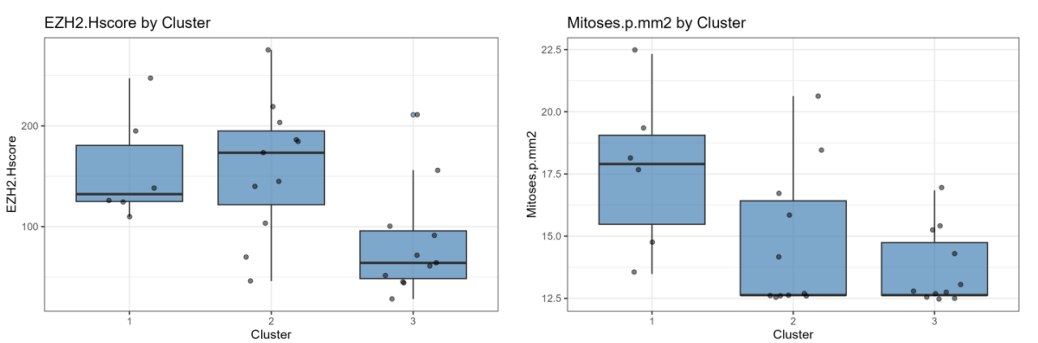

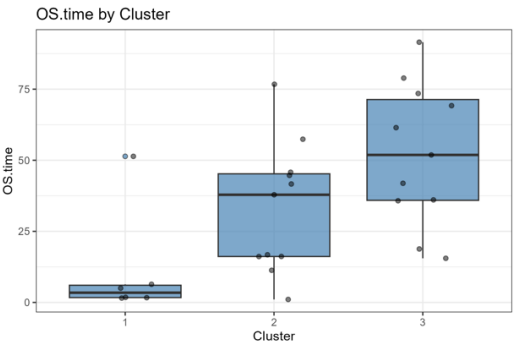

Figure 21. Box plots of the clinical variables comparing the clusters of grade 3 meningiomas. EZH2 score, mitotic index (mitosis count per mm^2) and overall survival per cluster in grade 3 are presented.

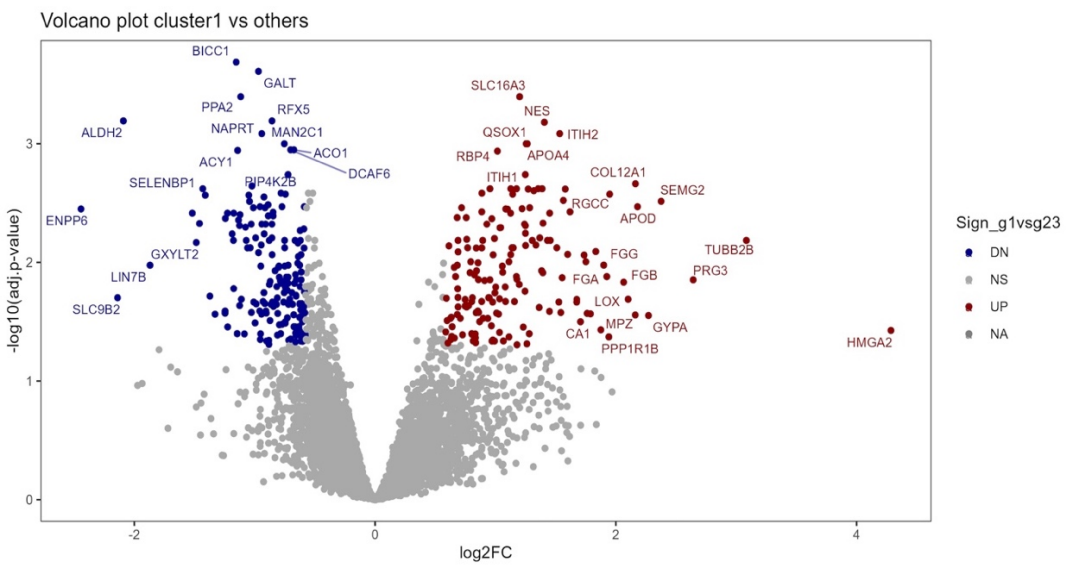

Figure 22. Volcano plot of differentially expressed proteins in cluster 1 vs clusters 2 and 3. Proteins to the right are the upregulated proteins in cluster 1, while proteins on the left are downregulated in cluster 1.

Figure 22 represents the differential protein expressions in cluster 1 vs clusters 2 and 3 within grade 3 meningiomas. In line with the heatmap patterns, cluster 1 contains a large number of both upregulated and downregulated proteins compared to the other two. Many highly expressed proteins in this cluster include plasma-associated proteins, such as APOA4, APOD, fibrinogen chains FGA, FGB, FGG, and extracellular matrix remodeling proteins, such as COL12A1, QSOX1, ITIH1 and ITIH2. Together, these proteins point toward strong extracellular matrix remodeling, coagulation and wound healing activity, which

are features commonly linked to an invasive phenotype. HMGA2 is also highly upregulated and represents an aggressive molecular marker, supporting the poor clinical outcome seen in this subgroup.

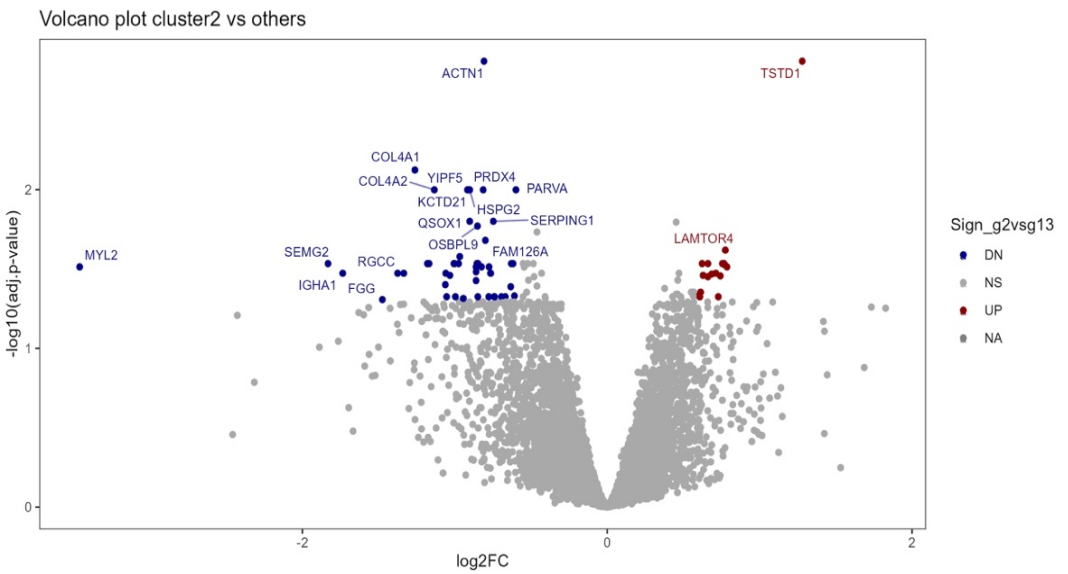

Figure 23. Volcano plot of differentially expressed proteins in cluster 2 vs clusters 1 and 3. Proteins to the right are the upregulated proteins in cluster 2, while proteins on the left are downregulated in cluster 2.

Figure 23 indicates that only a few proteins are significantly upregulated in cluster 2, including LAMTOR4, which is involved in amino acid sensing and activation of mTORC1, a pathway linked to cell growth. High level of this protein was related to poor survival in several cancers. (Gamallat et al., 2024) Another upregulated protein is TSTD1, involved in sulfur metabolism and redox homeostasis**,** often elevated in metabolically active tumor cells. These patterns suggest a more metabolic phenotype for this subgroup.

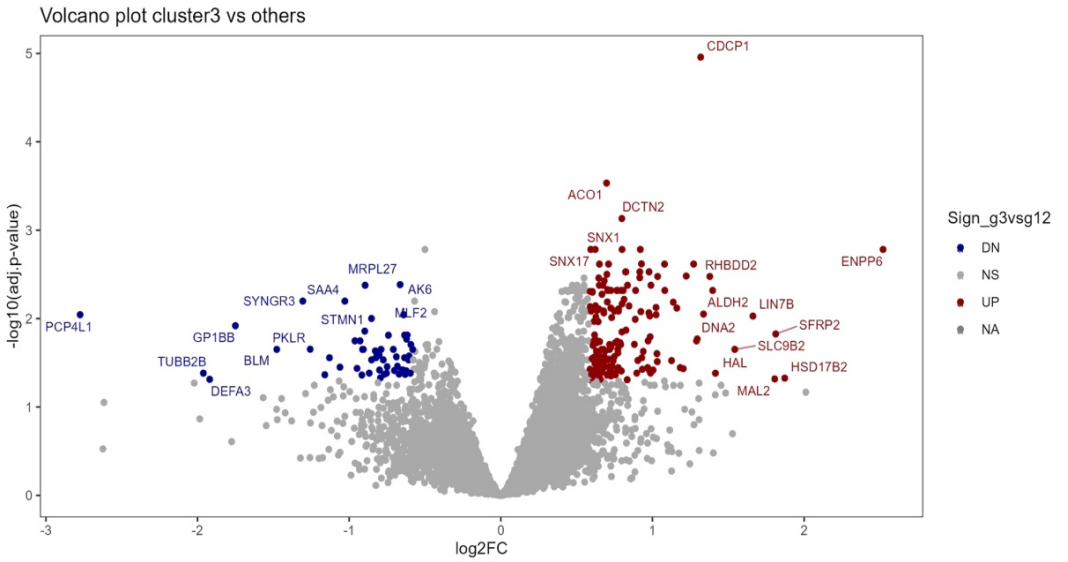

Figure 24. Volcano plot of differentially expressed proteins in cluster 3 vs clusters 1 and 2. Proteins to the right are the upregulated proteins in cluster 3, while proteins on the left are downregulated in cluster 3.

The volcano plot in Figure 24 presents the significantly differentially expressed proteins in cluster 3 as compared to cluster 1 and 2. This subgroup is characterized by proteins involved in endosomal trafficking (SNX1 and SNX17) and cell metabolic activities (ACO1, ALDH2 and HSD17B2), indicating a more regulated metabolic state. Interestingly, proteins such as DNA2, involved in DNA repair and replication, as well as SFRP2, involved in signaling modulation are also highly expressed in this subgroup. These findings may indicate that, despite being classified as WHO grade 3, tumors in this cluster could be biologically less aggressive than those in the other two clusters.

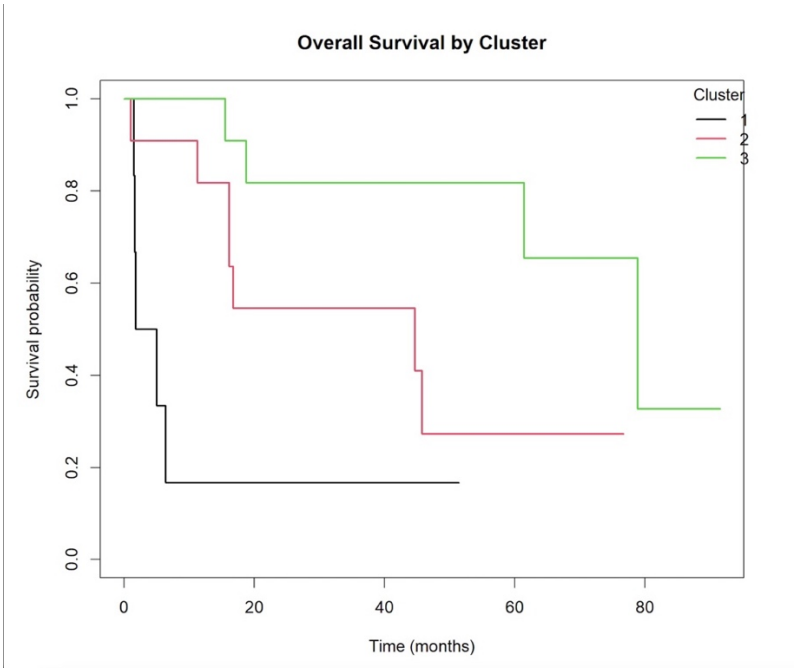

Figure 25. Kaplan–Meier overall survival curves for the three grade 3 proteomic clusters.

The results of the Kaplan – Meier overall survival analysis for the proteomic clusters within grade 3 meningiomas are presented in Figure 25. It can be noted that cluster 3 shows the best survival probability, with patients being alive for an average of 52,2 months and a much slower decline in survival over time compared with the other clusters. Tumors from this sample cluster appear to be less clinically aggressive. This is consistent with the proteomic profile of tumors in this cluster, which is dominated by more regulated biological processes. In contrast, cluster 1 shows the worst prognosis, with patients living on an average of only 11,3 months. This corresponds with the ECM remodeling features and strong tumor-microenvironment interactions observed in this subgroup, which might contribute to its highly aggressive nature and poor patient outcomes. Cluster 2 demonstrates an intermediate survival pattern, consistent with its proteomic characteristics. Overall, this results suggests that high-grade meningiomas are not only molecularly different but also biologically heterogeneous, with clear differences in clinical behavior between proteomic subgroups

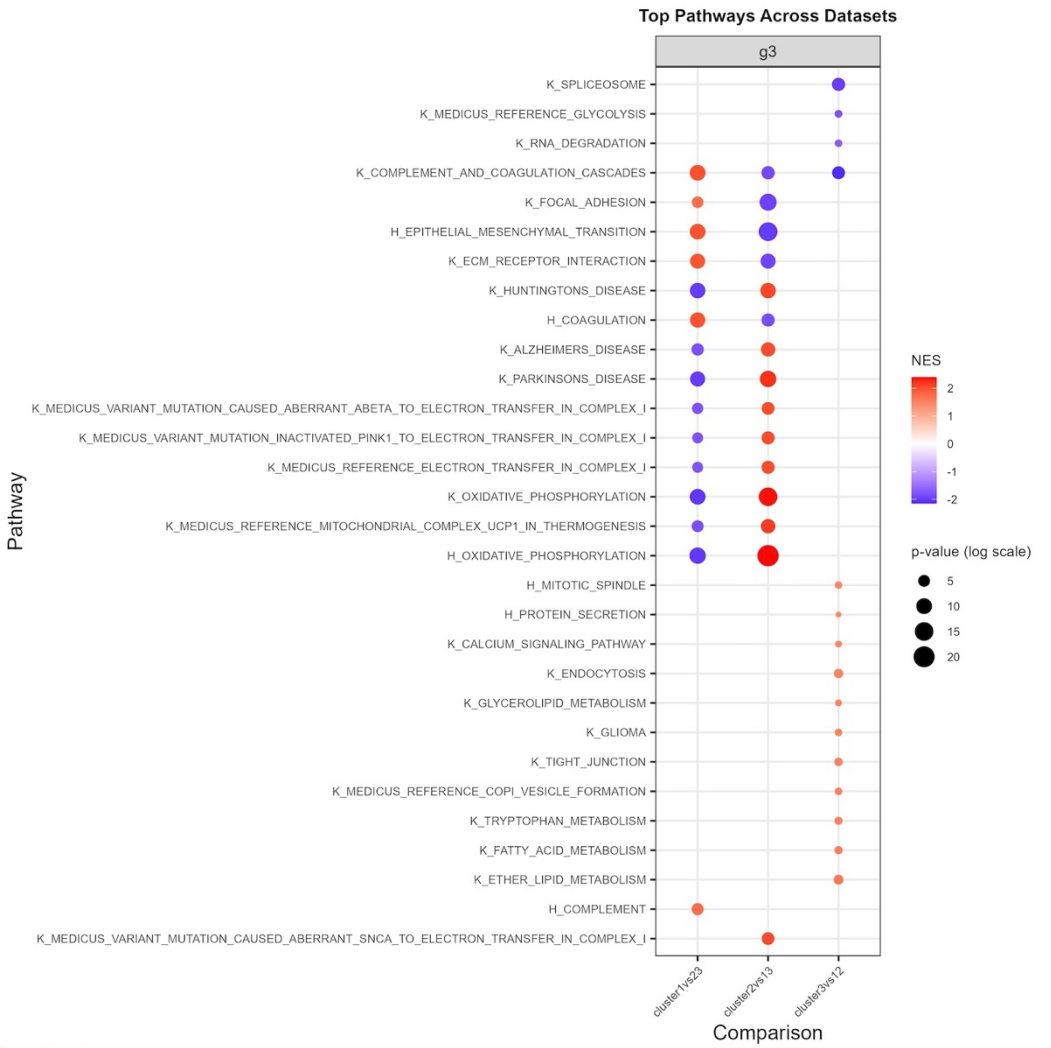

Figure 26. Most significant pathways across the 3 clusters within grade 3 meningiomas.

Figure 26 presents the gene set enrichment analysis summary of grade 3 meningioma clusters, where red is representing positive Normalized Enrichment Score (i.e. pathway upregulated in the specific cluster), while blue is negative NES (i.e. downregulated pathway in the specific cluster). In the first cluster the most upregulated significant pathways are those related to complement and coagulation cascades, focal adhesion, ECM receptor interaction, epithelial mesenchymal transition and coagulation. As it was seen previously from the volcano plot on a protein level in Figure 22, cluster 1 is dominated by wound healing and coagulation pathways as well as ECM remodeling pathways, which confirms the microenvironment driven and invasive phenotype of this cluster. In the second cluster, the most significant pathways are those related to oxidative phosphorylation and mitochondrial electron transport chain. Similar to the results

in Figure 23, these pathways show that this cluster is dominated by metabolic activity pathways, which are indicators of a cell intrinsic tumor state. Cluster 3 on the other hand is enriched with mitotic spindle pathways, RNA degradation, endocytosis, lipid metabolism, which are indicators of a controlled proliferation nature of this cluster, hence having the best survival outcomes. This pathways plot consolidates the protein level results seen in the volcano plots. It once again demonstrates how biologically distinct the meningiomas within the same grade can be and gives information on the prognosis based on the biology of these meningioma clusters.

Conclusion

This thesis has established and applied a robust proteomic workflow for FFPE meningioma tissues, which can be applied to any FFPE tissue types. This workflow was used to investigate protein expressions and proteomic differences between grade 1 and grade 3 meningiomas but also to explore the heterogeneity within grade 3 meningiomas. Associations with EZH2 protein expression were also in a focus within the analysis.

The primary outcome of the pilot optimizations was the development of a xylene-free FFPE tissue processing method for large cohorts. The EnVision deparaffinization method produced higher protein concentration at first, however the resulting lysates were cloudy and very difficult to handle and preserve the reproducibility, which in turn might affect accuracy. In contrast, the n-heptane/methanol protocol resulted in clear lysates, easy to handle, and enabled efficient high throughput processing. BeatBox and Bioruptor protein extraction methods resulted in similar protein yields, however the BeatBox had higher throughput and better reproducibility. For protein digestion methods, the magnetic bead-based digestion resulted in better peptide and protein identifications compared to the S-trap protocol. The automated KingFisher protocol without pre-equilibration, loading 50 µg proteins had the best balance between reproducibility, throughput and proteome depth.

The optimized workflow was finally applied to the meningioma cohort, which revealed clear proteomic differences between grade 3 and grade 1 tumors. Grade 3 meningiomas showed elevated levels of proteins associated with proliferation and metabolic activity, consistent with their higher tumor grade and more

aggressive nature. These results were reinforced by GSEA analysis, which displayed a strong enrichment of RNA processing and DNA replication pathways in grade 3 meningiomas, while pathways enriched in grade 1 meningiomas were more of a homeostatic nature, cytoskeleton organization and adhesion related processes. This indicated that grade 3 meningiomas are characterized by a more proliferative nature and increased biosynthetic activity as opposed to grade 1 being more characterized by tissue maintenance and lower activity.

This thesis also demonstrated that there is biological heterogeneity within grade 3 meningiomas. Hierarchal clustering revealed 3 subgroups of grade 3 meningiomas, exhibiting different clinical behaviors. Cluster 1 revealed enrichment of pathways involved in wound healing, coagulation, ECM remodeling, and proteins associated with strong microenvironment related phenotypes and tumor aggressiveness such as HMGA2. This cluster was also associated with the worst survival outcome. Cluster 2 was characterized by cell intrinsic pathways and with an intermediate survival rate. In contrast, cluster 3 displayed a more regulated molecular profile and displayed the highest survival rate of the 3 clusters.

EZH2 scores showed patterns consistent with proliferative features such as mitotic index, aligning with previous studies where EZH2 activity was linked to aggressive meningiomas.

This study has several implications. First, proteomic profiling offers a powerful approach to help improve the classification of meningioma patients beyond conventional histological grading. The identification of a microenvironment-driven high-risk cluster suggests potential therapeutic options by targeting the most significant pathways involved in that cluster. The identification of a grade 3 subgroup with better prognosis indicates that some patients might benefit from less intensive/agressive treatment strategies if robust molecular markers can be validated.

A limitation of this study is the cohort size, however, considering the rarity of grade 3 meningiomas, the dataset can still be considered meaningful. Future studies integrating spatial proteomics, transcriptomics, and clinical annotations will be essential to validate these subtypes and translate them into clinically actionable classifiers.

In summary, the results demonstrate that grade 3 meningiomas display distinct molecular states with different biology, proteomic signatures and prognosis. By moving beyond purely histological grading to pathway-level proteomic characterization, this work contributes to a deeper understanding of high grade

meningioma biology and provides a foundation for more precise biological stratification and therapeutic targeting.

References

Goldbrunner, R., Stavrinou, P., Jenkinson, M.D., Sahm, F., Mawrin, C., Weber, D.C., Preusser, M., Minniti, G., Lund-Johansen, M., Lefranc, F., Houdart, E., Sallabanda, K., Le Rhun, E., Nieuwenhuizen, D., Tabatabai, G., Soffietti, R. and Weller, M. (2021) EANO guideline on the diagnosis and management of meningiomas. *Neuro-Oncology*, **23**(11), pp. 1821–1834. https://doi.org/10.1093/neuonc/noab150

Humphries, E.M., Loudon, C., Craft, G.E., Hains, P.G. and Robinson, P.J. (2024) Quantitative comparison of deparaffinization, rehydration, and extraction methods for FFPE tissue proteomics and phosphoproteomics. *Analytical Chemistry*, **96**, pp. 13358–13370. https://doi.org/10.1021/acs.analchem

John M Elizarraras, Yuxing Liao, Zhiao Shi, Qian Zhu, Alexander R Pico, Bing Zhang, WebGestalt 2024: faster gene set analysis and new support for metabolomics and multi-omics, *Nucleic Acids Research*, Volume 52, Issue W1, 5 July 2024, Pages W415–W421, https://doi.org/10.1093/nar/gkae456

Kuras, M., Woldmar, N., Kim, Y., Hefner, M., Malm, J., Moldvay, J., Döme, B., Fillinger, J., Pizzatti, L., Gil, J., Marko-Varga, G. and Révész, M. (2021) Proteomic workflows for high-quality quantitative proteome and post-translational modification analysis of clinically relevant samples from formalin-fixed paraffin-embedded archives. *Journal of Proteome Research*, **20**(2), pp. 1027–1039. https://doi.org/10.1021/acs.jproteome.0c00765

Mayo Clinic (2019) *Meningioma – Diagnosis and treatment*. Available at: https://www.mayoclinic.org/diseases-conditions/meningioma/diagnosis-treatment/drc-20355648 .

Mayo Clinic (2024) *Meningioma – Symptoms and causes*. Available at: https://www.mayoclinic.org/diseases-conditions/meningioma/symptoms-causes/syc-20355643 .

Nassiri, F., Liu, J., Patil, V., Mamatjan, Y., Wang, J.Z., Hugh-White, R., Macklin, A.M., Khan, S., Singh, O., Karimi, S., Corona, R.I., Liu, L.Y., Chen, C.Y., Chakravarthy, A., Wei, Q., Mehani, B., Suppiah, S., Gao, A., Workewych, A.M., Tabatabai, G., Boutros, P.C., Bader, G.D., de Carvalho, D.D., Kislinger, T., Aldape, K. and Zadeh, G. (2021) A clinically applicable integrative molecular classification of meningiomas. *Nature*, **597**(7874), pp. 119–125. https://doi.org/10.1038/s41586-021-03850-3

Sahm, F., Bertero, L., Brandner, S., Capper, D., Goldbrunner, R., Jenkinson, M.D., Kalamarides, M., Lamszus, K., Albert, N.L., Mair, M.J., Berghoff, A.S., Mawrin, C., Wirsching, H.G., Maas, S.L.N., Raleigh, D.R., Reifenberger, G., Schweizer, L., Suwala, A.K., Tabatabai, G., Tabouret, E., Short, S., Wen, P.Y., Weller, M., Le Rhun, E., Wesseling, P., van den Bent, M. and Preusser, M. (2025) European Association of Neuro-Oncology guideline on molecular testing of meningiomas for targeted therapy selection. *Neuro-Oncology*, **27**(4), pp. 869–883. https://doi.org/10.1093/neuonc/noae253

Sahm, F., Schrimpf, D., Stichel, D., Jones, D.T.W., Hielscher, T., Schefzyk, S., Okonechnikov, K., Koelsche, C., Reuss, D.E., Capper, D., Sturm, D., Wirsching, H.G., Berghoff, A.S., Baumgarten, P., Kratz, A., Huang, K., Wefers, A.K., Hovestadt, V., Sill, M., Ellis, H.P., Kurian, K.M., Okuducu, A.F., Jungk, C., Drueschler, K., Schick, M., Bewerunge-Hudler, M., Mawrin, C., Seiz-Rosenhagen, M., Ketter, R., Simon, M., Westphal, M., Lamszus, K., Becker, A., Koch, A., Schittenhelm, J., Rushing, E.J., Collins, V.P., Brehmer, S., Chavez, L., Platten, M., Hänggi, D., Unterberg, A., Paulus, W., Wick, W., Pfister, S.M., Mittelbronn, M., Preusser, M., Herold-Mende, C., Weller, M. and von Deimling, A. (2017) DNA methylation-based classification and grading system for meningioma: a multicentre, retrospective analysis. *The Lancet Oncology*, **18**(5), pp. 682–694. https://doi.org/10.1016/S1470-2045(17)30155-9

Salu, P. and Reindl, K.M. (2025). Agr2 in cancer and beyond: unraveling its role during protein synthesis, ER stress, and as a predictive biomarker. *Molecular and Cellular Biochemistry*, [online] 480(10), pp.5205–5219. doi:https://doi.org/10.1007/s11010-025-05318-8.

Szőke, P., Sztankovics, D., Dankó, T., Mohammed, A.A., Váncza, L., Papp, G., Márk, Á., Bödör, C., Sebestyén, A., Dezső, K. and Scheich, B. (2025) EZH2 overexpression is associated with aggressive behavior and promotes cell proliferation in CNS WHO grade 3 meningiomas. *Neuro-Oncology Advances*, **7**(1), vdaf112. https://doi.org/10.1093/noajnl/vdaf112

Tyanova, S., Temu, T., Sinitcyn, P., Carlson, A., Hein, M.Y., Geiger, T., Mann, M. and Cox, J. (2016). The Perseus computational platform for comprehensive analysis of (prote)omics data. *Nature Methods*, 13(9), pp. 731–740. https://doi.org/10.1038/nmeth.39

Wang, J., Landry, A., Raleigh, D., Sahm, F., Walsh, K., Goldbrunner, R., Leeor Yefet, Tonn, J., Gui, C., Ostrom, Q., Barnholtz-Sloan, J., Perry, A., Ellenbogen, Y., C Oliver Hanemann, Jungwirth, G., Jenkinson, M., Tabatabai, G., Mathiesen, T., Mcdermott, M. and Tatagiba, M. (2024). Meningioma: International Consortium on Meningiomas (ICOM) consensus review on scientific advances & treatment paradigms for clinicians, researchers, and patients. *Neuro-Oncology*, 26(10). doi:https://doi.org/10.1093/neuonc/noae082.

Appendix

Final protocol

Deparaffinization (heptane + methanol)

Set up the thermoblock to 37°C.

1. Add 510µL heptane and 90 µL methanol in all the sample tubes.
2. Incubate in the thermomixer at 37°C for 10 min with mixing/shaking at 900rpm.
3. Centrifuge at room temperature for 5 min, 15000g.
4. Remove the solvent and let air dry for 5 min, or until the samples dry out completely.(take notes on the tissue pieces)

Protein extraction (beat box)

5. At the same time set the boiling temperature to 95°C so the thermomixer has time to heat up when it's time to use it.
6. Load the dry tissues in the beat box plate. (Add 50µL lysis buffer(TRIS), to help with the loading of the tissues so they don't fly away. Use pincets). Add another 50µL LB after loading the samples.
7. Place the plate in the beatbox for 15 min(High). Repeat another 15 min cycle.
8. Centrifuge the whole plate for 30-60 sec at 500g.
9. Place the plate in the metal plate so that the metal beads stick to the sides. In that way it's easier to take the lysate out.
10. Transfer all the liquid in the corresponding tube where the tissues were initially, then boil them in the thermomixer for 1 hour at 95°C.
11. Open and close the lids carefully after 5-10 minutes and again after 20-30 minutes to release pressure and to prevent evaporation.
12. Centrifuge for 10 min, 20000g.

Label tubes(0.6 tubes) for the protein determination the next day. Depending on the tissue sample sizes:

- 10x dilution→ 3µL lysate+ 27µL water
- 5x dilution→ 6µL lysate + 24µL water

Calculate how much lysis buffer needed
200µL per sample → 43 samples so around **9ml**

	Stock	Conc. needed	Dilution	Amount needed
TRIS-HCl	1M	100mM	10x	900µL

SDS	20%	4%	5x	1800µL
DTT	500mM	10mM	50x	180µL
Water				6120µL

Protein determination (Pierce 660nm assay)

1. Dilute standard (BSA 2mg/mL) 2x(because highest point is 1000), starting at 1:1 (40 µL water + 40 µL BSA). Vortex and spin between every dilution. Add range(1000 to 62,5)
2. Dilute samples 1:10 (3 µL sample + 27 µL water). Vortex and spin. (depends on piece of tissue, diluted concentration should be within range)
3. Make the working reagent (20 mL Protein assay reagent + 1 sachet Ionic detergent compatibility reagent(1g)). Vortex and wrap it with foil (*photoreactive!*). → depending on how many samples we have, for example if there are 5 standards, 1 blank and 6 samples, with two replicates so (5+1+6) x 2 = 24. We need 150 µL in each so in total we need 3600 uL or around 4 ml to be safe. For 4 ml we need 0.2 g of the white powder or 200ug.

- For the real samples:
- 2 blanks + (4x2) standards(125-1000) + 43x2 samples = 96 x 150 =14400. Prepare around 16000uL. For 16 ml we need 0.8g of the ionic reagent.

4. Pipette standards, blank (MILIQ water) and samples (10 µL) in the plate (*all in duplicates!).*
5. Pipette working solution (150 µL) into the plate.
6. Cover the plate with the lid.
7. Shake the plate for 10s at 500 RPM and incubate at RT for 5 minutes (dark). In case i have to remeasure it should be done within 15min!
8. Set up the plate on the computer:
    - *test set up -> protocol* (choose method)
    - *plate layout* (set up standards, blank and samples)
    - *measure -> measure -> sample ID/dilution factors* (set up dilutions)
9. Insert the plate into the plate reader as soon as the incubation time ends and press *start measurement* when ready.
10. Press wizard and check the curve. Add raw data, blank correction, and sample ID before linear regression (concentration µg/mL) and export data to USB in excel file.

Digestion (King Fisher)

1. **Sample + IAA + Lysis buffer has to equal 50µL.**
2. **Lysis buffer**→ 1 ml needed.
    - 100mM TRIS + 4% SDS + 10mM DTT + water

	Stock	Conc. needed	dilution	Amount needed
TRIS	1M	100mM	10x	100µL
SDS	20%	4%	5x	200µL
DTT	500mM	10mM	50x	20µL
Water				680µL

3. **Digestion buffer needed for Plate 8**
    - For the real samples we need 250uL x 46 = 11500 µL digestion buffer.(11.5 ml)
    - Stock has to be 0.1 µg/µL.
    - Trypsin ratio → 1:25
    - Lys C ratio → 1:100.
    - Trypsin conc→ 1/250=0.004 uµg/µL → 25x dilution
    - Lys C cons→ 0.25/250=0.001 µg/µL → 100x dilution
    - Trypsin amount→460 uL trypsin stock (0.1µg/µL)
    - Lys C amount→ 115 uL(0.1µg/µL).
    - We need 50 mM TEAB. Stock is 1000mM so it's a 20x dilution (1000/50). 11.5 ml/20 =**600 µL from the stock** + **10.9ml water**
4. Add **250 µL digestion buffer** in each well
5. Prepare **plates 2-4 with 100% ACN**, **1000µL in each well**
6. Prepare **plates 5-6 with 70% EtOH**, **1000µL in each well**
7. Add the respective sample according to the table in each well + **2µL IAA** + **Lysis Buffer** so that it adds up to 50µg per well.
8. Add **10µL of magnetic beads** to each well.
9. Add **140µL of 100%ACN** in each well right before putting the plate in the King Fisher instrument.